Memoirs of the Faculty of Engineering, Nagoya University
Vol. 40, No. 1 (1988)

STUDY ON THE PERFORMANCE OF WATER THERMAL STORAGE

NOBUO NAKAHARA, KAZUNOBU SAGARA*,
MAKOTO TSUJIMOTO and MASAYA OKUMIYA

Department of Architecture

(Received May 31, 1988)

Abstract

Theoretical development and a practical design process, accompanied with easy-to-apply data, are introduced in three parts for some representative and practical types of water thermal storage tanks. The first part describes basic design concepts, system composition and controls, characteristics of the most popular multi-connected complete mixing tanks, and the practical estimation table of storage efficiencies of this type.

In part 2, a theoretical mixing model was developed for the temperature-stratified type of thermal storage water tank. Empirical equations consisting of the model parameter and input conditions were derived from a number of experiments under the stepwise temperature input. The model was further extended to be applied to various input conditions. The effects of various design parameters on storage efficiency were examined statistically with experimental designs through numerical simulations, which resulted in estimation tables of the storage efficiency of this type.

In part 3, it is revealed that a self-balanced type of stratified tank, which is composed of main tank and subheaders that accept returned chilled/heated water, maintains stable stratification regardless of the type of imposed inlet condition. The performance was tested by experiment and compared with numerical simulation results. An estimation table consisting of two-level factors was prepared through system simulation with the help of design of experiment as introduced in the two preceding parts, and was made comparable with the simple temperature-stratified tanks as described in part 2.

---

* Mie University, Department of Architecture

Introduction

Japanese thermal storage for HVAC actually began in Tokyo in 1952, designed by M. Yanagimachi.[1] He proved the economic advantages of the technology, flexibility of operation, and effective utilization of energy as well as energy conservation, but he never tried to provide any usable design data for engineers. Nakahara[2] analyzed the operational results of an actual thermal storage tank and proposed a disturbance factor for the design of multi-connected tanks based on temperature profiles of the tank and gave an estimation table of storage efficiency using a "temperature difference ratio" (explained later) as an index (Nakahara[3]). Nakajima[4] and Matsudaira et al.[5] paid attention to the dynamic response of the outlet temperature of the tank corresponding to a stepwise temperature and/or thermal input. Nakajima developed his logic based on the mixing-diffusion model in which M value was applied as the mixing character. Matsudaira constructed his model as a combination of complete mixing and piston flow without any diffusion and exhibited step responses for several tanks in series and various ratios of the piston flow zone to the complete mixing zone. He proposed a storage efficiency defined as stored heat in the tank vs. total heat input at the time of unit water change in the step response. The problems with these studies are that (1) attention was focused on the outlet response for stepwise input only, preventing them from understanding the nonlinearity of the mixing process in the tank; (2) they did not identify thermal responses of tanks in any real situation with their models; and (3) they never tried to provide any practical design data that enabled prediction of the storage efficiency. At the same time, they did not notice the grave effects of the secondary (HVAC) system characteristics on storage performance. Tamblyn evaluated alternatives for resisting temperature blending in 1980 and arrived at the "moving baffle" concept (Tamblyn[6]). This excellent idea seemed to have some difficulties in relating hardware to baffle installation, compared to an empty tank, and the absolute value of separation itself is obscure. The authors established standard types of water thermal storage (Nakahara et al.[7]), have constructed the mathematical model through many experiments and actual experiences, and have established the predictive methodology of storage performance, which practical engineers can apply with ease. An outstanding feature of the authors' design method is that it is based on the temperature profile analysis, which also led to optimal controls in operation (Nakahara[8]), and that the statistical examination, as well as an estimation based on the "design of the experiment," was applied.

Water thermal storage is used for both cooling and heating. As the principle is the same for both cases, cooling will be used as the representative in the following description. For heating, temperature relation should be considered reversely.

Three parts of this paper have disclosed basic design concept and three measures to establish high efficiency thermal storage with piston flow characteristics.

Part 1. Basic Design Concept and Estimation of Storage Efficiency of Multi-Connected Complete Mixing Tanks

1. Basic Design Concept

Temperature Profile

The temperature profile method is the most convenient one to use to explain the

design and control concept of water thermal storage systems. Tanks are divided into several sections in the direction of the water flow, and temperature profiles are obtained by plotting the temperature of each section and connecting the plots. The greater the number of sections, the more precise the profile. This profile provides the following information:

1. The density of thermal storage is easily understood by the magnitude of the temperature difference.
2. The thermal capacity is easily calculated by the area covered by the profile.
3. Storage efficiency can be easily calculated, as described later in this paper.
4. The thermal behavior of the tank is understood, as well as problems to be solved.
5. The insulation performance is roughly calculated using the temperature shift during times of no thermal input/output.

Fig. 1 shows some examples of temperature profiles of multi-connected complete mixing tanks and single-temperature stratified tanks. Shadowed areas indicate the thermal input/output during the time interval T_i-T_j.

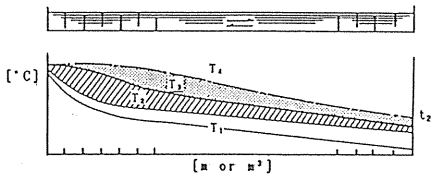

(a) Multi-Connected Complete Mixing Tanks

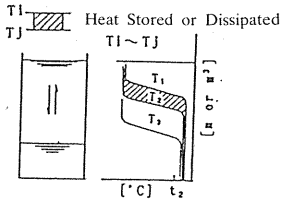

(b) Single Temperature Stratified Tank

Fig. 1. Temperature profile.

Storage Efficiency

Generally, efficiency means the ratio of output energy to input energy. In water thermal storage, degradation only occurs from heat loss by heat transference through walls and floors. In this sense, efficiency merely contributes to an increase in the capacity of the heat-generating plant. Therefore, the efficiency is unimportant in designing the tank and never contributes in determining the volume of the tank, so another kind of efficiency is defined in the present papers.

Tank volume is determined as follows: In Fig. 2, $Q(t)$ includes the heat loss of the HVAC system except a storage tank. Corresponding to the operation time of the heat generator, stored heat or the heat load to be stored in the tank, H_s, is obtained as shown in the figure. For the total daily load, H, including heat loss of the storage tank, the heat-generating capacity, G, is calculated as,

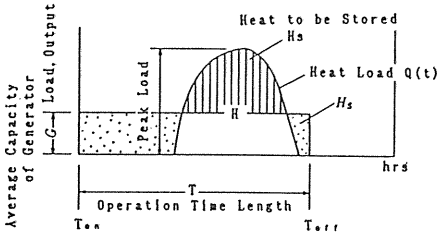

Fig. 2. Example of storage operation mode.

$$G=\frac{H}{T\cdot\varepsilon} \tag{1}$$

The generator means the chiller in the cooling condition and the heat exchanger, boiler, or heat pump in the heating season. Tank volume is calculated as

$$V=\frac{H_s}{c\rho\eta_s\Delta\theta_0}=\frac{H_s}{c\rho\Delta\theta_e} \tag{2}$$

where storage efficiency is defined as

$$\eta_S = \frac{H_S}{c\rho\,\Delta\theta_0 V} = \frac{(H_S/c\rho\,\Delta\theta_0)}{V} = \frac{V_0}{V} \tag{3}$$

V_0 is the nominal volume to store the heat, H_S, in the water tank with $\Delta\theta_0$ of nominal temperature difference. Thus, storage efficiency is thought to be defined in volumetric sense and also is the ratio of actual stored heat vs. nominal stored heat, or the maximum possible stored heat available in water volume, V, with nominal temperature difference, $\Delta\theta_0$. It should be noted that the product of η_S and $\Delta\theta_0$ determines the tank volume. Thus, $\Delta\theta_e$ or $\eta_S \cdot \Delta\theta_0$ is called the effective temperature difference of the thermal storage tank. Fig. 3 shows the difinition and calculation procedure of storage efficiency, η_S.

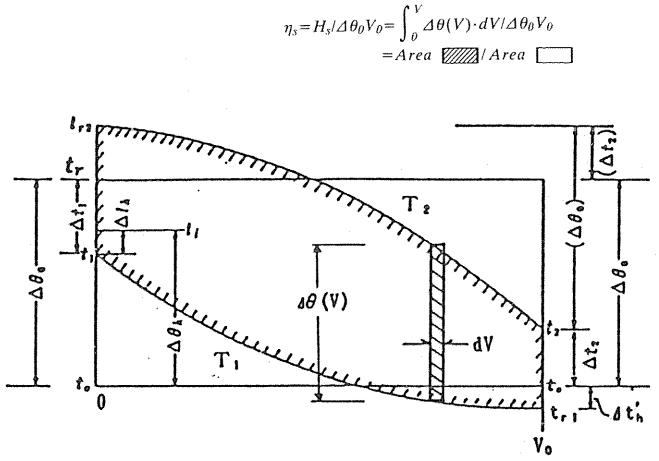

LTDR: Limit Temperature Difference Ratio

$\frac{\Delta t_1}{\Delta\theta_0}$: $LTDR_1$, Dimensionless Limit Temperature Difference referred to Generator Inlet Temperature and Coil Temperature Difference

$\frac{\Delta t_1}{\Delta\theta_h}$: $LTDR_h$, Dimensionless Limit Temperature Difference referred to Generator Inlet Temperature and Generator Temperature Difference

$\frac{\Delta t_2}{\Delta\theta_0}$: $LTDR_2$, Dimensionless Limit Temperature Difference referred to the Allowance of HVAC Coil

Fig. 3. Definition of storage efficiency.

The following facts are easily understood referring to the figure and Eq. (3).

1. The nominal temperature difference, $\Delta\theta_0$, should be large. This means that the water temperature difference in the heat-exchanging coil in air conditioners should be large. This also required less pump power.
2. The distance between the maximum profile (or terminal profile) at time T_2 and the minimum profile (or initial profile) at time T_1 should be large.
3. Higher profile at time T_2 and/or lower profile at time T_1 enlarge the area, A, and results in higher storage efficiency. This means that a higher allowable delivery (chilled) water temperature, t_2, to the AC circuits and a lower allowable inlet temperature, t_1, to the heat generator (refrigerating machine) are preferred, because they result in a higher temperature of return water from the AC circuit and lower chilled water from the refrigerating machine into the tnak. This could result in trade-off relations, in which the rows of cooling coils may increase and the COP of chillers may slightly decrease.

The value η_s changes with the definition of $\Delta\theta_0$. In order to easily follow the design procedure, $\Delta\theta_0$ is defined here as the temperature difference through the coil at the time of peak air-conditioning loads, as described in Eq. (4).

$$\Delta\theta_0=\frac{\sum_i \Delta\theta_i Q_i}{\sum_i Q_i} \tag{4}$$

The limit temperature differences, which are defined as t_2-t_0 for the HVAC side or secondary circuit and t_r-t_1 for the refrigerator side or primary circuit, respectively, are divided by $\Delta\theta_0$ to make a dimensionless number called the limit temperature difference ratio, LTDR. The meaning of LTDR is discussed later.

System Composition

The authors' experiences recommend a standard piping and control diagram as shown in Fig. 4. Advantageous variations are as follows, providing the water level is higher than the pump position (See Fig. 6):

1. Possible failure in water suction due to absorbing air can be avoided.
2. All inlets and outlets to and from these tanks interfacing primary and secondary circuits can be unified without any trouble due to the difference of water pressure between inlets at the three-way valve in the suction line.

In Fig. 4(a) the most important measure in the primary circuit is to install a three-way control valve at the suction line manipulated by the outlet temperature of the chiller, in order to keep the temperature of the lowest temperature part of the tank, to be referred to hereafter as the first tank, as near as possible to the set-point temperature of generators. PID is the desired control action for avoiding offset. Capacity control should be done by electrical current, so that generator capacity is kept in a full state. The sensor for controlling the three-way valve also sends an OFF-signal to the generator. An ON-signal is sent to the generator by sensors in the storage tank, which can estimate the magnitude of heat stored through either an automatic (Nakahara[8]) or a manual learning process. Refer also to explanations in Fig. 4(a).

Three variations are shown in Fig. 4(b) for the secondary circuit diagram: variable flow rate system with two-way valve control (VWV), constant flow rate system with three-way valve control (CWV), and no control for coil load, either with (Fig. 4(b) 3) or without (Fig. 4(b) 2) constant delivery temperature control (CDT) for CWV and no

§ Explanation of (a)

1. Inlet vane of heat pump shall be controlled by electric current to assure full output.
2. Outlet temperature of heat pump shall be controlled by adjusting inlet temperature to heat pump with mixing highest temperature water and lowest temperature water in tank, to keep constant outlet temperature in full output.
3. Control action of mixing three way valve is preferred using PID to avoid offset. Usually electro-pneumatic system is applied.
4. Off-signals for heat pump shall be given by the same controller as outlet temperature controller to avoid interaction due to errors of sensing elements. Optimal control is preferrred more (Nakahara 1981).
5. On-signals for heat pump is preferred to be given by water temperature of appropriate position in tank. The position shall be searched for during operating experience. Optimal control is preferred more (Nakahara 1981).

(Ⓡ is supposed as heat pump in chilling mode.)

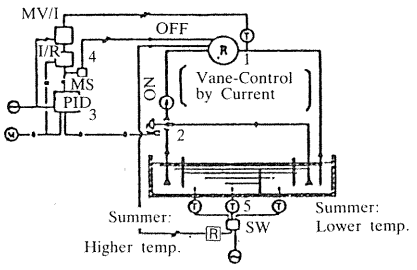

(a) Primary Circuit (Heat Source)

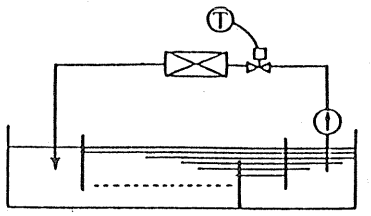

① VWV, 2-way Valve Control

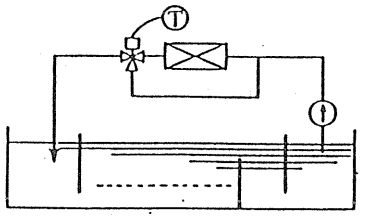

② CWV, 3-way Valve Control

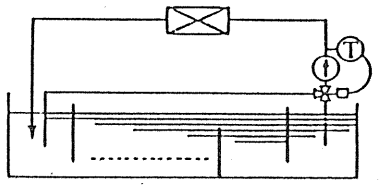

③ CWV for Coil, VWV for Tank and 3-way Valve Control at Pump Suction (Constant Delivery Temperature Control, CDT)

(b) Secondary Circuit (HVAC System)

Symbols:

Ⓣ : Temperature Sensor
⊖ : AC Current Source
Ⓜ : Main Air Source for Pneumatic Control
Ⓡ : Relay
SW : Turn over Switch
MV/I : Millivolt/Current Converter
I/R : Current /Pneumatic Converter
MS : Monitor Switch

Fig. 4. Standard control system for water thermal storage system.

control. VWV does not request CDT, and it is most desirable from the viewpoint of higher storage efficiency and energy conservation as well. When the use of either or both CWV and no control is unavoidable, DCT control can raise the efficiency considerably, as well be seen later.

Prototype Storage Tanks

The authors recommend three types of standard prototype storage tanks[9] for the sake of maintaining higher thermal storage efficiency. These are the multi-connected complete mixing tanks, temperature stratified tanks and self-balanced temperature stratified tanks.

2. Mixing Model

The multi-connected complete mixing tanks usually consist of more than 10 tanks, preferably more than 15, to avoid the dead space in the tank and to maintain a reasonable storage efficiency. The inlets and outlets of each tank should be alternately located at top and bottom and right to left to reduce any possible dead space. The temperature difference between the neighboring two tanks is then less than one degree and the inflow velocity is relatively high, so that the incoming fluid mixes rapidly, even under buoyant inflow conditions, because the Archemedean number, which is the most influential dimensionless number in the buoyant flow field (see Part 2), is very small. ("Buoyant inflow conditions" refers to higher temperature input at a top tank position into lower temperature tank water, or the reverse. On the contrary, higher temperature inflow at the bottom position into lower temperature tank water, or the reverse condition, shall be called the "mixing inflow condition".) When the inlet Archimedean number, Ar_{in}, is small or negative, the tank condition becomes complete mixing with very little dead space. See part 2 of these reports about a quantitative analysis of the matter (Nakahara et al.[10]). Some preferred allocations of connecting pipes are illustrated in Fig. 6.

Thus, each of the multi-connected tanks can be assumed as having a complete mixing property. Tsujimoto et al. substantiated this by comparing the actual measurement with a calculated result, as shown in Fig. 5, for 26 serially connected tanks with a volume of 1350 m^3 (Tsujimoto et al.[11]). However, when a very low flow rate in the tank occurs at a certain time during simultaneous operating of both the primary and the secondary circuit, or at a low heat load in the VWV system with only the secondary circuit

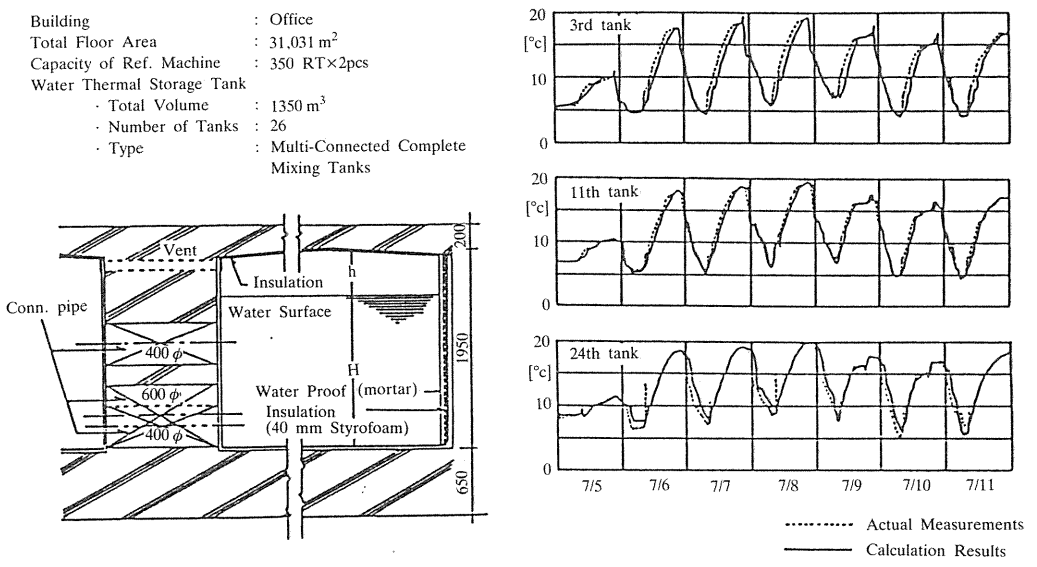

Fig. 5. Comparison between actual measurements and calculation results as multi-connected complete mixing tanks (Tsujimoto, et al.).

operation, a little dead space may occur. Therefore, it is preferable to apply approximately 95% of the effective capacity rate as a safety factor, judging from Fig. 5 and the authors' past experience. This kind of safety factor is called the effective volume ratio, P, which is exact in a volumetric sense but different from η_s. These two should not be confused. The nature of P would be easily understood by imagining the temperature-stratified hot water tank with both inlet and outlet at the top position. Most of the lower part of that tank is dead and never contributes to thermal storage, resulting in values of P far less than 0.95 in this case.

3. Simulation Program

Fig. 6 shows a simplified system diagram and variations in tank prototypes, inlet/outlet composition, and controls in both the primary and secondary circuits. Solar

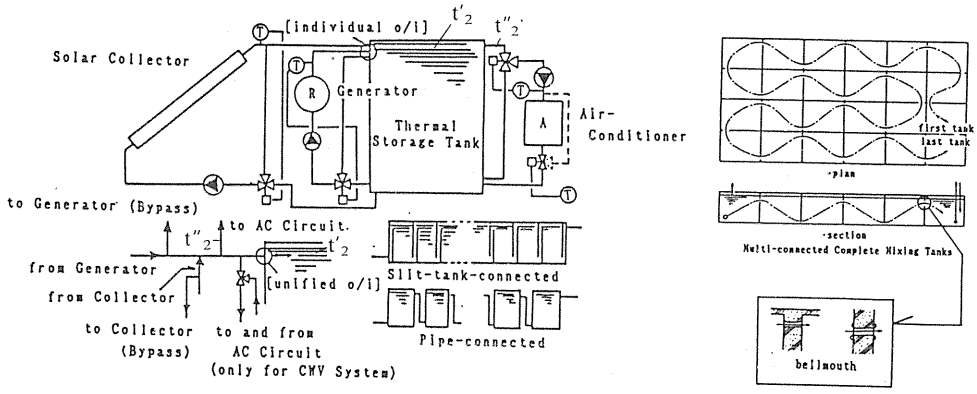

Fig. 6. HVAC system diagram with water thermal storage for system simulation.

collectors can be provided for both cooling and heating. The simulation program is divided into three parts, as shown in Fig. 7, taking the memory size of the 16-bit microcomputer into consideration. The program was written in Basic and compiled by an MS-MOS Basic compiler before computation. (Another program in Fortran can be utilized for either the multi-connected complete mixing tanks or the temperature-stratified tanks.)

The first part of the program is assigned to system information inputs, heat load input, calculation of generator capacities and the water flow rate of both the primary and secondary circuits, the primary calculation of the tank volume, and the time step for computation.

The second part of the program is the water temperature simulation during 24 hours of system operation. The algorithm for the multi-connected complete mixing tanks is that of the first-order lag system, as shown in Eq. (5), and its finite difference form in Eq. (6). The temperature, θ_{in} or θ_{i-1}, is that of the tank upstream of the tank, i, and V is the

volume of a single tank.

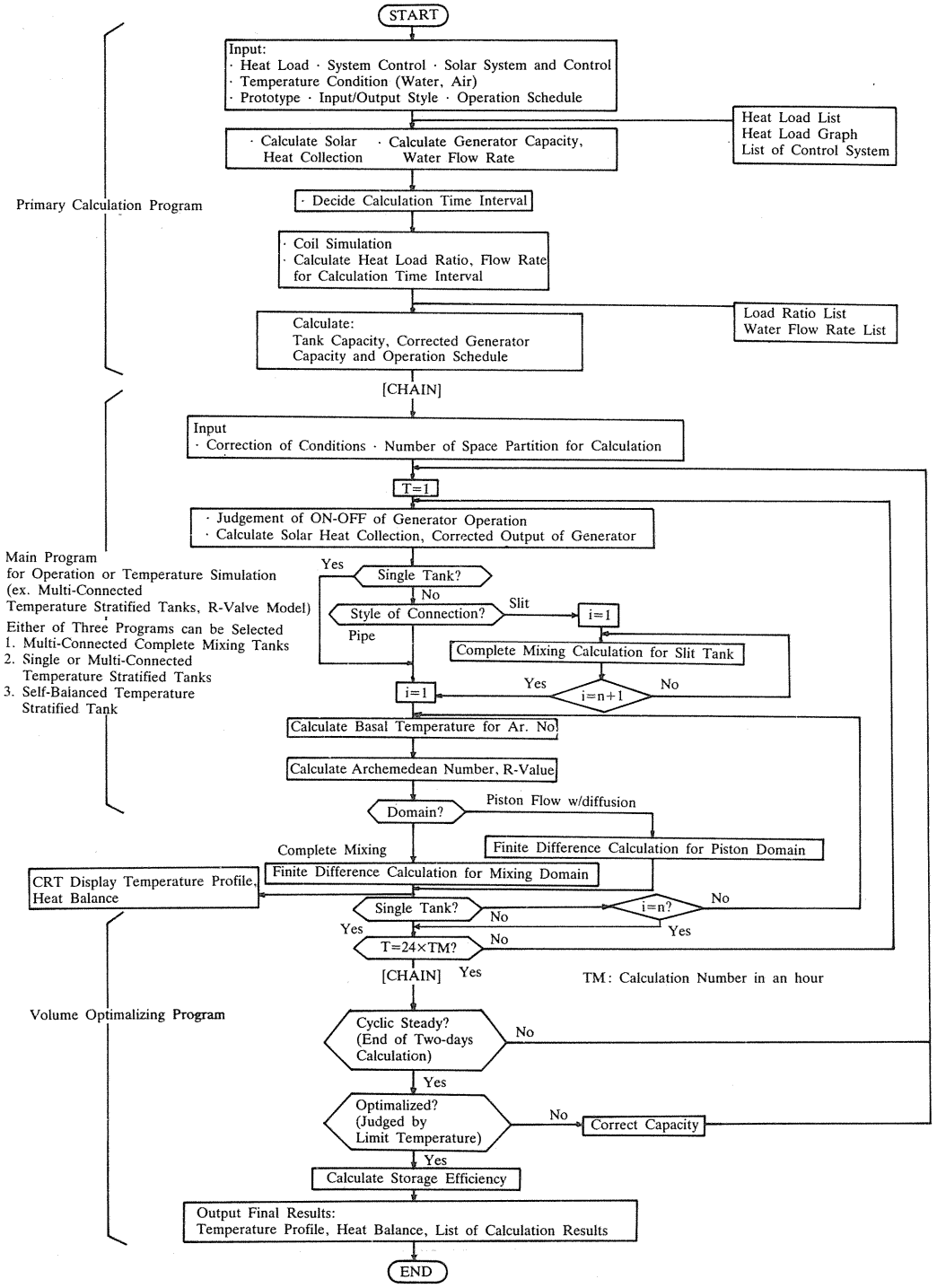

Fig. 7. Flow chart of system simulation program for water thermal storage system.

$$V\frac{d\theta}{dT}=Q(\theta_{in}-\theta)+\frac{q_{loss}}{c\rho} \tag{5}$$

$$\theta_{i,T}=\theta_{i,T-1}+\frac{\Delta T}{V}\left[Q(\theta_{i-1,T-1}-\theta_{i,T-1})+\frac{q_{loss,T}}{c\rho}\right] \tag{6}$$

The heat balance in the first and the last tank is a little different from Eq. (6) because of outflow and/or inflow to and from the system. For example, in the case of a charging process with simultaneous discharge in unified and individual I/O, as shown in Fig. 6, for the fist tank, Eq. (6) is varied to Eq. (7) and Eq. (8), respectively, from heat balance.

Unified I/O:

$$\theta_{1,T}=\theta_{1,T-1}+\frac{\Delta T}{V}\,Q(\theta_c-\theta_{1,T-1})+\frac{q_{loss,T}}{c\rho} \tag{7}$$

Individual I/O:

$$\theta_{1,T}=\theta_{1,T-1}+\frac{\Delta T}{V}\,Q_R(\theta_c-\theta_{1,T-1})+\frac{q_{loss,T}}{c\rho} \tag{8}$$

Thus, slightly different results are suggested between unified and individual I/O, even in the case of the complete mixing prototype. The heat loss or gain, q_{loss} and/or Q_{loss}, should be small from the viewpoint of the recommendation of the prototype. Strict calculation of it needs instationary algorithm and convergence procedure and consumes much computation time with little contribution. Therefore, the daily heat loss was assumed as constant and calculated from the difference between approximate mean water temperature and environmental temperature. Refer to the manual calculation example in Fig. 12.

The third part of the program is for adjusting the tank volume to an optimal one. First, let the calculation continue for the second day in order to obtain a steady-state solution. Second, the secondary limit temperature, t_2 is examined and the change in volume, either an increase or a decrease, is calculated from the temperature profile, and the program is chained again to the main program with a new tank volume. After several adjustment procedures, using the Newton-Raphson method from the second iteration onward, an optimal tank volume is obtained together with the storage efficiency and effective temperature difference. This adjusting process may be handled manually if desired.

4. Examination, Estimation of Factorial Effects

Design of Experiment

With a process as complicated as water thermal storage, the combination of "design of experiment" and system simulation plays a valuable role in finding out significant factors, identifying the significant factorial effect quantitatively, and estimating any

required effect for arbitrary combination of significant factors. In this way, not only can one estimate the value for any selected case, but he can arrive at an optimal answer in designing the system he confronts. The first trial of this methodology for the HVAC field in Japan was made by Yokoyama et al.[12] in identifying effects of conditions such as insulation thickness of walls, building window size, design room temperature, etc., on annual heating and/or cooling load for the sake of energy conservation.

Suppose eight factors may affect the storage efficiency. If three levels of estimation are supposed, 3^8 experiments should be executed. Yet, the precision is insufficient because of the lack of iteration for each case. If one uses the orthogonal array by design of experiment, 81 experiments, or simulations, are enough to achieve precise examination of significance for each factor. The rquired effect, storage efficiency in this case, for example, is calculated by summing all the factorial effects and total mean value. Moreover, the confidence interval can be known, and interactive effects of some pairs of factors are also given. The reader is referred to the details in the literature (Taguchi[13]; Connor et al.[14]). The important premise is that the computerzied system simulation should replace the real experiment, which means the system model and algorithm of calculation should be reliable.

Choice of Factors and Levels

Even with the orthogonal array, a large number of factors needs a large array, which will result in much computation time. Referring to Figs. 3, 4, and 6 and explaniations about them, the following factors were selected for discussion.

1. Limit temperature difference ratio (LTDR): The qualitative effects are clear in Fig. 3. The extreme limit is determined by the lowest allowable outlet temperature of chillers and the highest allowable inlet temperature to air-handling units.

   The two kinds of LTDR on the higher temperature side indicate the following: The primary LTDR, LTDR1, relates to the difference of design temperature condition between the HVAC coil outlet and the inlet of the evaporator. The generator LTDR, $LTDR_h$, relates to the lowest allowable water temperature for the chiller operation.
2. Heat load pattern: Heat load pattern was considered to affect the changing mode of temperature profiles interactive with valve control mode and thus affect the performance of water thermal storage. Therefore, three levels of heat load pattern were assumed, as shown in Fig. 8.
3. The ratio of minimum heat load vs. maximum heat load (Min./Max.): The ratio was assumed the same for both the CWV and VWV systems. This factor may affect the storage efficiency due to the partial heat load and has s grave effect on the temperature profile, because the water temperature returning to the tank varies greatly (Fig. 8).

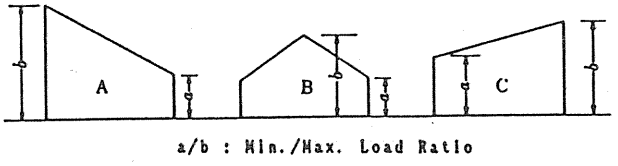

Fig. 8. Heat load pattern.

4. CWV heat load ratio: This is the ratio of the daily heat load of the CWV systems to the total daily load.

These two factors, 3 and 4, are clearly interactive. It should be noted that the flow rate to and from the storage tank is constant, but the temperature difference is proportional to the heat load in the CWV systems with three-way valve control. But for the VWV systems with two-way valve control, the flow rate is far less than proportional to the heat load and the temperature difference is far larger than constant. Thus, the effects on temperature profiles of these two types of control systems should appear different by combining the Min./Max. of the load pattern and the CWV heat load ratio. This situation is shown in qualitative terms in Fig. 9. If the load pattern is flat, the difference between the CWV system and the VWV system dissipates.

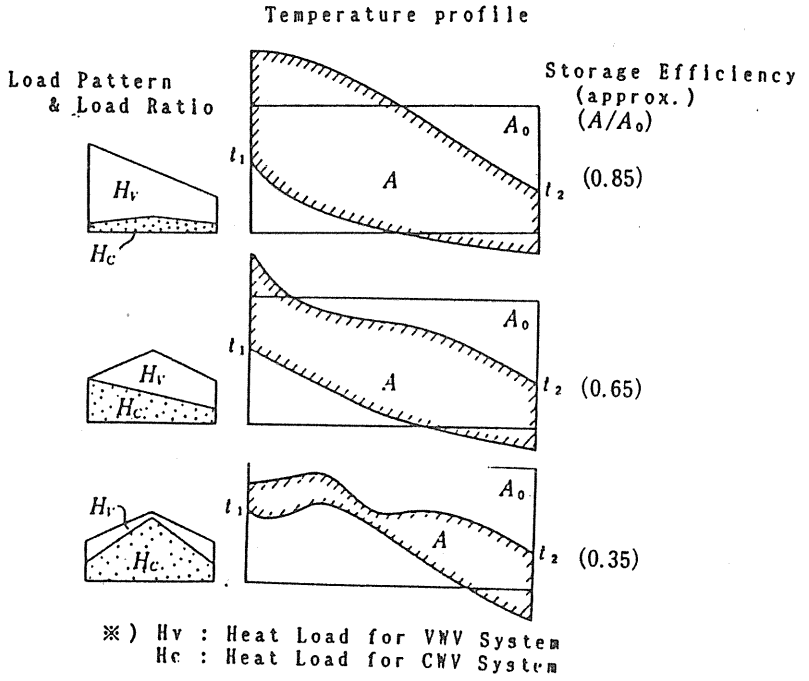

Fig. 9 Effect of heat load ratio and heat load pattern.

5. Number of tanks: As mentioned before, a single tank can be supposed to be complete mixing but th piston flow characteristics as a whole would appear more with the increase in the number of tanks, which should raise the storage efficiency.
6. Operation schedule of generators: The effect of this factor may appear due to the overlapping of the primary and secondary circuit operations, which has the effect of keeping the first tank, from which the water is sent to the secondary circuit, always at a low temperature during overlapping, resulting in

the terminal temperature profile being moved toward the low temperature side. This increases the storage capacity.

7. Constant delivery temperature control (CDT): The adverse effect of the CWV system, which causes temperature profiles to fall, can be offset by applying constant delivery temperature control, as shown in Fig. 4(b). From the authors' experience, the most undesirable situation for water thermal storage is when the percentage of heat load handled by a fan/coil unit system with a low temperature difference is dominant. Even if the heat load ratio is not so great, the water flow rate greatly increases due to the low temperature difference of the fan/coil units, which usually have no flow control on the water side. In this case, water thermal storage performance drastically decreases. Sometimes the storage tank becomes totally useless, even harmful. This is where CDT control may provide the remedy.
8. Inlet/outlet style (I/O style): As shown in Fig. 6 and Eqs. (7) and (8), whether the inlets and outlets to and from the first and last tank are unified or not must somewhat affect the behavior of water temperature due to mixing. Moreover, in the case of unified I/O style, water to the secondary circuit before the three-way mixing valve (cf., t_2' in Fig. 6 and Fig. 11) is drawn from the primary circuit, of which the temperature is kept low at t_0, with priority to or from the first tank in which temperature varies more. This results in the water temperature in the first tank (cf., t_2'' in Fig. 6 and Fig. 11) rising higher than the design limit temperature, t_2 for delivery.
9. Interactions: Some factors may be affected by the level of other factors. For example, the disadvantage of the CWV system disappears if the Min./Max. ratio of heat load is unity. This kind of interactive effect is examined and evaluated with the analysis of variance (ANOVA) and compensates for the principal factor effect as follows in an estimation process. For the above-mentioned case, the principal effect of the former $[CWV]_j$, that of the latter $[MINMAX]_k$ and their interactions $[CWV \cdot MINMAX]_{j \cdot k}$, are added to each other and results in the synthesized effect as $[CWV]_j = [MINMAX]_k + [CWV \cdot MINMAX]_{j \cdot k}$. The j and k mean the levels chosen for the corresponding factor.

Allocation on Orthogonal Array

An orthogonal array and interaction table between rows are prepared elsewhere (Taguchi[13]). $L27(3^{13})$ means 27 experiments for 13 factors of three levels. In other words, 3^{13} experiments are reduced to 27 with the $L27(3^{13})$ orthogonal array. However, the interactive effect of two factors appears in two rows, and a few pairs of interactions often appear in the same row, which results in confounding among them. In addition, rows allocated for errors are needed in order to efficiently examine significances by ANOVA. In the present subject, approximately 10 factors and several interactions required at least $L81(3^{40})$, which seemed a reasonable scale for simulation execution.

Allocation to the orthogonal array, execution of the system simulation as experiments, and ANOVA were conducted for the first time using all of the factors described above, except the CDT and I/O style (Nakahara et al.[15]). The results showed that the heat load pattern, the Min./Max. ratio of heat load for the VWV system, and the generator LTDR were statistically insignificant. Other experiments (Sagara et al.[16]) showed that the CDT and the I/O style had considerable significance, especially for the

former one, in the case of the temperature stratified tank (See part 2). Therefore, all the significant factors in the first experiments, CDT and I/O style were chosen as the factors for the second experiments, as shown in Table 1. The levels are also listed in the table. As the process of allocation is not easy when the array becomes as large as L81, it was computerized. Simulations were carried out for all 81 combinations.

Table 1. Factors and levels for design of experiment.

	Factors	Levels		
		I	II	III
A	Operation Schedule of Generator (Schedule)	0:00–24:00	7:00–22:00	22:00–8:00
B	Min./Max. Ratio of Daily Heat Load (Min./Max.)	0.8	0.5	0.2
C	Existence of Constant Delivery Temperature Control for CWV System (CDT)	No	Yes(1)*1	Yes(2)*2
D	Daily CWV Heat Load Ratio to to Daily Total Heat Load (CWV Ratio)	0.2	0.5	0.8
E	Limit Temperature Difference Ratio for Primary Side (LTDR1)	0.4	0.6	0.8
F	Limit Temperature Difference Ratio for HVAC Side (LTDR2)	0.2	0.4	0.6
G	Number of Tanks (N)	10	20	40
H	Inlet/Outlet Style (I/O Style)	Unified	Individual	Mixed*4

*1. Delivery temperature=design temperature of inlet water to coil
*2. Delivery temperature=design temperature of inlet water to coil $\pm$*3$0.2\times$(temperature difference through coil)
*3. positive for cooling, negative for heating
*4. unified style at the first tank and individual style at the last tank

Table 2. Results of ANOVA.

Factors	Storage Efficiency				
	SS	DF	MS	F_0	ρ(%)
	$\times10^{-4}$		$\times10^{-4}$		
A	4268	2	2134	36.3**	6.0
B	1565	2	782	13.3**	2.1
C	19586	2	9793	166.5**	28.1
D	6229	2	3115	53.0**	8.8
E	4988	2	2492	42.4**	7.0
F	18093	2	9047	153.8**	25.8
G	965	2	483	8.2**	1.2
B×D	672	4	168	2.9*	0.6
C×D	3518	4	880	15.9**	4.7
C×E	2459	4	615	10.5**	3.2
C×F	3014	4	754	12.8**	4.0
B×F	1396	4	349	5.9**	1.7
e	2350	40	59		6.8

Note. SS : Sum of Squares
DF : Degree of Freedom
MS : Mean Square (Unbiased estimate of variance)
F_0 : F distribution
ρ : Contribution
** : 1% of significance
* : 5% of significance

Results

Calculated data for 81 cases by the system simulation program described were analyzed and the significance of factors, including interactions, on the storage efficiency were examined. Then an estimation table consisting of those factors with a significance rate of 5% or better was prepared. Table 2 is the final result of ANOVA after pooling insignificant factors and interactions into error in order to raise a testing power. Estimation of storage efficiency and/or effective temperature difference is possible using Table 3.

Table 3. Estimation tables of storage efficiency η_s for multi-connected complete mixing tanks.

Factor		$\eta_s=1.136+\Sigma\ \Delta\eta i$			Levels		
		Factorial Effects $\Delta\eta i$			I	II	III
		I	II	III			
A** : Schedule		−0.018	0.097	−0.078	0−24	7−22	22−8
B** : Min./Max.		0.046	0.013	−0.059	0.8	0.5	0.2
C** : CDT		−0.209	0.047	0.163	No	Yes(1)	Yes(2)
D** : CWV Ratio		0.124	−0.057	−0.067	0.2	0.5	0.8
E** : $LTDR_1$		−0.106	0.023	0.083	0.4	0.6	0.8
F** : $LTDR_2$		−0.157	−0.044	0.201	0.2	0.4	0.6
G** : N		−0.043	0.042	0.002	10	20	40
		D_1	D_2	D_3			
	B_1	−0.051	0.016	0.035			
B×D*	B_2	0.023	−0.012	−0.035			
	B_3	0.028	−0.028	0.000			
		F_1	F_2	F_3			
	B_1	0.030	−0.007	−0.022			
B×F**	B_2	0.050	−0.044	−0.006			
	B_3	−0.080	0.051	−0.028			
		D_1	D_2	D_3			
	C_1	0.121	−0.095	−0.026			
C×D**	C_2	−0.035	−0.026	0.009			
	C_3	−0.086	0.070	0.017			
		E_1	E_2	E_3			
	C_1	−0.105	0.027	0.077			
C×E**	C_2	0.037	−0.012	−0.025			
	C_3	0.068	−0.015	−0.053			
		F_1	F_2	F_3			
	C_1	0.049	−0.121	0.072			
C×F**	C_2	−0.020	0.058	−0.038			
	C_3	−0.030	0.064	−0.034			

Note 1. ** 1% of Significance
* 5% of Significance
2. Confident interval for mean value=±0.102%

Principal effects of storage efficiency are graphically shown in Fig. 10 in order to be understandable intuitively and visually. It should be noted that significance is not absolute, but relative. If strong significant factors exist in the range of the three levels, comparatively weak significant factors dissipate as insignificant. The I/O style was of this kind and had a weak significancy, less than 5%, in which the unified I/O was shown preferable. Therefore, it is necessary to set up reasonable, that is, practical, levels for each factor.

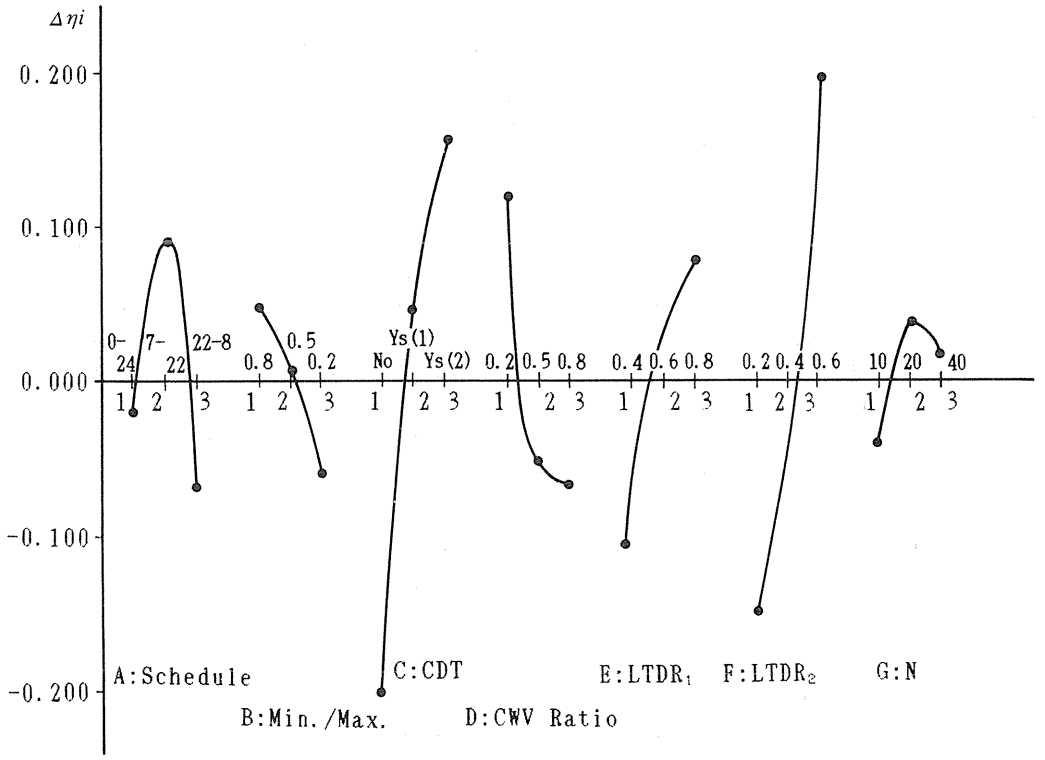

Fig. 10. Factorial main effects.

The only factor showing characteristics of the tank structure itself is the number of tanks, G, which produces comparatively small effects. To the contrary, system design parameters contribute greatly to the storage efficiency, as represented by two kinds of limit temperature differences, E and F, and the cooling/heating water coil inlet/outlet temperature setting. In addition, the temperature control systems, such as the factors C, D and F have a grave effects as expected. It can be said that some extent of disadvantage due to heat load pattern B, operation schedule A, and tank structure G, which are often out of the engineer's control, could be cancelled out by skilled design.

In order to examine the degree of variation, see Fig. 11 for the three simulation results. Design conditions and combinations of levels for significant factors are written in the figure, as well as some characteristic values. The values in parentheses are those estimated from Table 2 for comparison with simulated values.

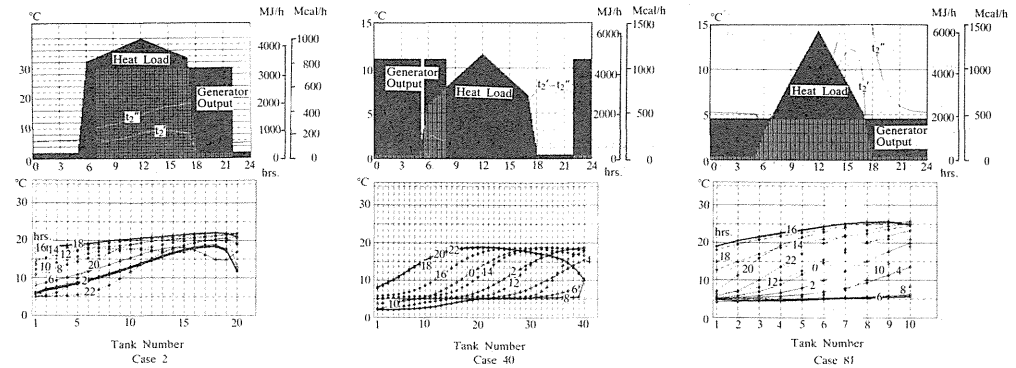

(a)

Experimental Condition: $A_2\ B_1\ C_1\ D_2\ E_1\ F_2\ G_2\ (H_2)$
Storage Efficiency ηs
Computed: 0.623
Estimated: 1.136+0.097+0.046−0.209
−0.057−0.106−0.044+0.042
+0.016−0.007−0.095−0.105−0.121
=0.596
G: 3232 MJ/h (772 Mcal/h)
t_1: 12.2°C
t_2: 9.8°C
t_0: 5°C
t_i: 17°C
$\Delta\theta_0$: 12°C
Hd: 46057 MJ (11000 Mcal)
Hs: 12691 MJ (3031 Mcal)
V: 405 m^3

(b)

Experimental Condition: $A_3\ B_2\ C_2\ D_3\ E_2\ F_1\ G_3\ (H_3)$
Storage Efficiency ηs
Computed: 0.964
Estimated: 1.136−0.078+0.013+0.047
−0.067+0.023−0.157+0.002
−0.030+0.050+0.009−0.012−0.020
=0.916
G: 4849 MJ/h (1158 Mcal/h)
t_1: 9.8°C
t_2: 7.4°C
t_0: 5°C
t_i: 13°C
$\Delta\theta_0$: 12°C
Hd: 46057 MJ (11000 Mcal)
Hs: 38123 MJ (9105 Mcal)
V: 787 m^3

(c)

Experimental Condition: $A_1\ B_3\ C_3\ D_1\ E_3\ F_3\ G_1\ (H_1)$
Storage Efficiency ηs
Computed: 1.532
Estimated: 1.136−0.018−0.059+0.163
+0.124+0.083+0.201−0.043
+0.028−0.028−0.086−0.053−0.034
=1.414
G: 2022 MJ/h (483 Mcal/h)
t_1: 7.4°C
t_2: 9.8°C
t_0: 5°C
t_i: 9°C
$\Delta\theta_0$: 12°C
Hd: 46057 MJ (11000 Mcal)
Hs: 21538 MJ (5144 Mcal)
V: 280 m^3

Note: t_2':Suction temperature of the lower side to delivery pump to HVAC coils maximum value of $t_2'=t_2$
t_2'':The temperature of the first tank
$t_2''=t_2'$ at individual I/O style at the delivery side of secondary circuit
(cf. Figure 6)

Fig. 11. Temperature profiles and storage efficiencies for three case.

5. Design Method

Finally, Fig. 12 is the flow chart and an example of calculation of the manual design method of a water thermal storage system using the estimation table. Interpolation is preferred for any intermediate value of levels for continuous nature of factors, but extrapolation should be limited to only the nearby point of both ends. The procedures will be easily understood following the flow chart. A problem often experienced in Japanese practice is that the sufficient volume cannot necessarily be obtained because tanks consist of the space under the basement floor and are structurally determined. Feedback and several repetitions are necessary as shown in the figure.

The computation example (a) in Fig. 11, which is not unusual in actual design, shows a poorly designed case because the efficiency is rather low due to unfavorable selection of factor levels. When engineers follow a conventional way of designing systems without water thermal storage, this situation occurs and they may lose their reputation. The estimation table prepared here will assist them in obtaining successful results similar to those in case (b) or (c). It should be noted that the technology to increase efficiency in water thermal storage is mostly parallel with energy conservation methodology as already introduced by Nakahara.[17]

The design method introduced here is common for the three parts, except for the estimation table because of the different characteristics of each prototype.

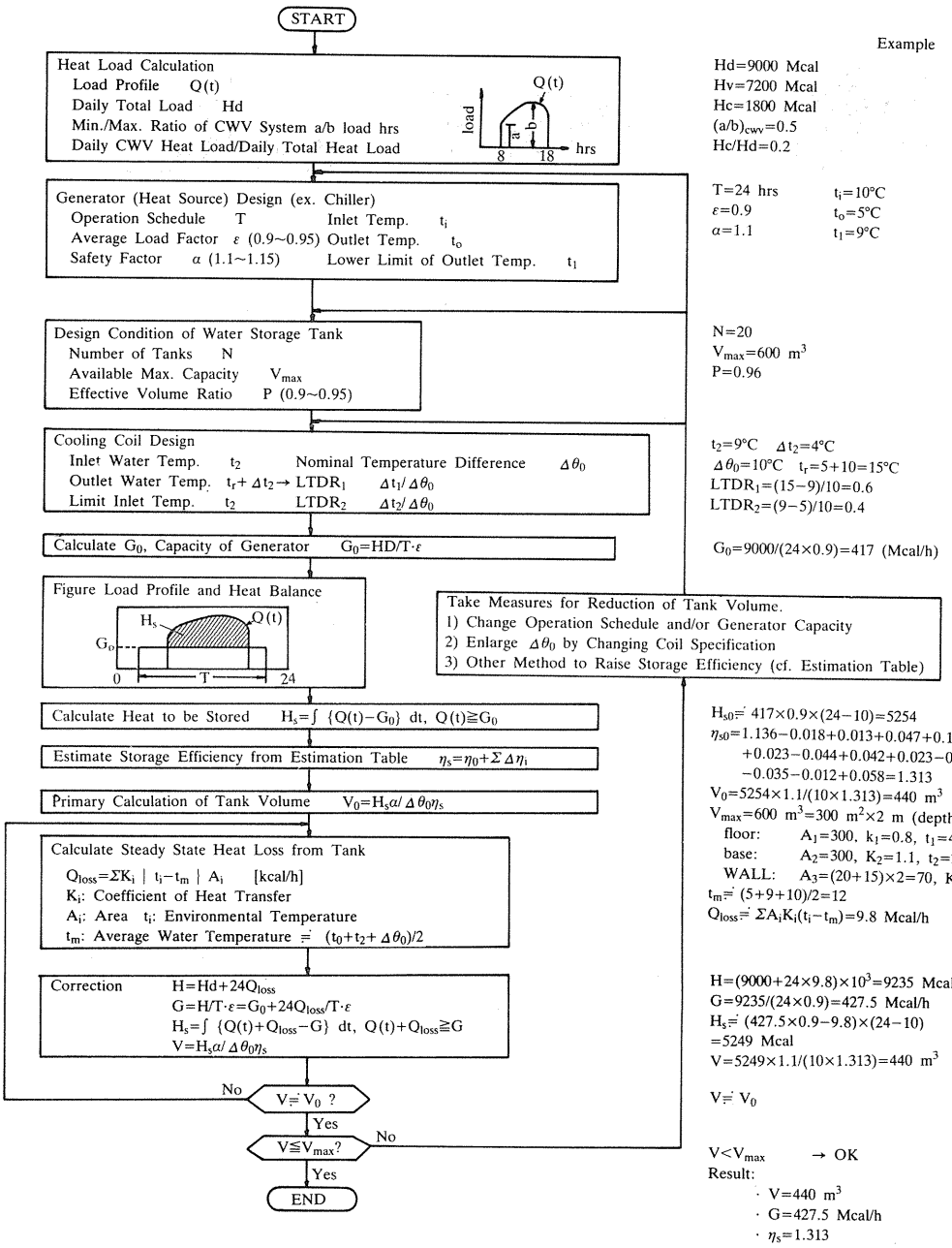

Example

Hd=9000 Mcal
Hv=7200 Mcal
Hc=1800 Mcal
$(a/b)_{cwv}=0.5$
Hc/Hd=0.2

T=24 hrs $t_i=10°C$
$\varepsilon=0.9$ $t_o=5°C$
$\alpha=1.1$ $t_l=9°C$

N=20
$V_{max}=600\ m^3$
P=0.96

$t_2=9°C$ $\Delta t_2=4°C$
$\Delta\theta_0=10°C$ $t_r=5+10=15°C$
$LTDR_1=(15-9)/10=0.6$
$LTDR_2=(9-5)/10=0.4$

$G_0=9000/(24\times0.9)=417$ (Mcal/h)

$H_{s0}\fallingdotseq 417\times0.9\times(24-10)=5254$
$\eta_{s0}=1.136-0.018+0.013+0.047+0.124$
$+0.023-0.044+0.042+0.023-0.044$
$-0.035-0.012+0.058=1.313$
$V_0=5254\times1.1/(10\times1.313)=440\ m^3$
$V_{max}=600\ m^3=300\ m^2\times2$ m (depth)
floor: $A_1=300$, $k_1=0.8$, $t_1=40$
base: $A_2=300$, $K_2=1.1$, $t_2=20$
WALL: $A_3=(20+15)\times2=70$, $K_3=0.8$, $t_3=20$
$t_m\fallingdotseq(5+9+10)/2=12$
$Q_{loss}\fallingdotseq\Sigma A_iK_i(t_i-t_m)=9.8$ Mcal/h

$H=(9000+24\times9.8)\times10^3=9235$ Mcal
$G=9235/(24\times0.9)=427.5$ Mcal/h
$H_s\fallingdotseq(427.5\times0.9-9.8)\times(24-10)$
$=5249$ Mcal
$V=5249\times1.1/(10\times1.313)=440\ m^3$

$V\fallingdotseq V_0$

$V<V_{max}$ → OK
Result:
· $V=440\ m^3$
· $G=427.5$ Mcal/h
· $\eta_s=1.313$

Fig. 12. Manual design process of water thermal storage system.

Part 2. Mixing Model and Estimation of Storage Performance of Temperature Stratified Tanks

1. Mixing Model

The simplest model of thermal response for a water storage tank is the complete mixing type, in which inflow water is assumed to mix instantaneously in the tank and thereby the temperature in the tank remains uniform. On the other hand, the mixing process in the temperature-stratified storage tank is suppressed due to strong buoyancy, resulting in high temperature in the upper portion of the tank and low temperature in the bottom. Therefore, modeling of the thermal response of the tank is reduced to the problem of estimating the buoyant effect in the mixing process.

A stepwise input of higher temperature water from the top inlet forms a horizontal buoyant jet at first, colliding against the opposite wall and then changing direction. The downward flow after the collision stops at a depth where the buoyant effect balances with its downward momentum. A temperature-stratified layer is formed near the depth, and its horizontal temperature distribution becomes nearly uniform. The stratified layer moves downward subsequently as thermal charge proceeds. This process was confirmed in a visualized experiment. Fig. 13 shows the process schematically.

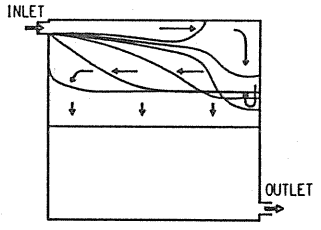

Fig. 13. Transitional behavior of inflow water in the temperature stratified storage tank with progress of thermal charge by a visualized experiment using dye.

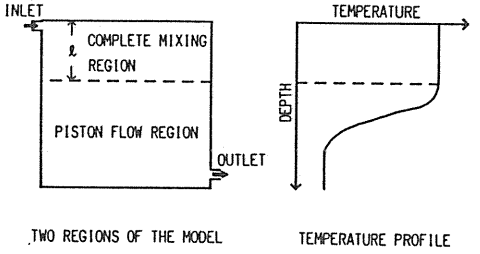

Fig. 14. Two regions of the mixing model for the temperature stratified storage tank.

Model Construction

The facts suggest that the mixing process in the stratified tank consists of two stages; the forming of a stratified layer and the transporting of that layer downward. This process was also pointed out by Yoo et al.[18] It is, therefore, assumed that the storage tank is divided into two regions; a complete mixing region increasing with the progress of thermal charge, and a piston flow region with one-dimensional diffusion as shown in Fig. 14.

According to the combined model of the two regions described above, a mathematical model with the equations shown below may be introduced.

$$\theta_{T+\Delta T}=\theta_{in}-(\theta_{in}-\theta_T)\exp\left(\frac{Q\,\Delta\,T}{VR}\right) \tag{9}$$

$$R=l/L=l_0/L+R_k T^*=R_0+R_k T^* \tag{10}$$

$$\frac{\partial\theta}{\partial T}=\varkappa\frac{\partial^2\theta}{\partial z^2}-U\frac{\partial\theta}{\partial z} \tag{11}$$

Eq. (9) corresponds to the complete mixing region, where R is the dimensionless depth of the region and increase linearly with dimensionless time, T^*, as described in Eq. (10). T^* is defined as $\int QdT/V$ (number of water exchanges). Eq. (11) corresponds to the piston flow region with one-dimensional diffusion, where U is downward water velocity at the cross section of the tank and is zero below the outlet. Initial temperature in the tank is uniform. The boundary conditions at both sides of the piston flow region are a complete insulated condition with no heat flux at the downstream end and the temperature of complete mixing region at the upstream end, respectively. The model ignores heat exchange between the tank walls and water.

The l in Eq. (10) is the depth of the complete mixing region, and its initial value is l_0. It should be noted that l_0 is hypothetical and obtained from the regression analysis of output response using the model described in Eqs. (9), (10), and (11). Therefore, the region is not actually formed at the beginning of input. This is the reason that the calculated temperature profile in the tank at the early stage does not coincide with a real profile until the stratified layer has formed. Oppel et al.[19] proposed a model using variable eddy conductivity as a smooth function in which its value is large at the inlet side and small at the outlet side. It is assumed in our model that its value is infinite up to the inlet side of the stratified layer, which results in a complete mixing region, and is a level of molecular conductivity at the outlet side, which results in a piston flow region, and that the infinite conductivity region increases with the progress of thermal charge.

It should be noted that l_0 (or R_0) is a main parameter in this mixing model. If l_0 as well as R_k are identified through experiments, the performance of any storage tank of this type can be estimated. Since it was thought that many conditions affect the value of l_0, the effects of input conditions and geometric conditions on the l_0 value were checked under various conditions.

2. Experiment

Apparatus

The tested storage tank was an 0.8 meter cube made of transparent acrylic resin, which permits high visibility. Other dimensions were realized by connecting basic units or by dividing with an insulated partition according to the demand. The tested tank was covered with 40 mm foam styrene insulation board, excluding the visualized experiments. A schematic diagram of the experimental setup is shown in Fig. 15(a). Heat loss through the tank side wall is confirmed to be less than 1% of input heat by preliminary

measurements using a heat flux meter.

Temperatures were measureed and recorded by 0.3 mm copper-constantan thermocouples positioned at the points in the tank shown in Fig. 15(b) and at the inlet and outlet as well. Ten sets of lead wires of thermocouples for the measuring points shown in the plan of Fig. 15(b) were led through nine 15 mm acrylic resin pipes filled with fine sand to prevent heat conduction along the lead. The tips of the thermocouples were coated with epoxy resin for electrical insulation. Preliminary experiments showed that a pipe installed for measurements nearest the inlet affected the inflow and the formation of the stratified layer in high flow rate cases, and so it was excluded in these cases to prevent the disturbance.

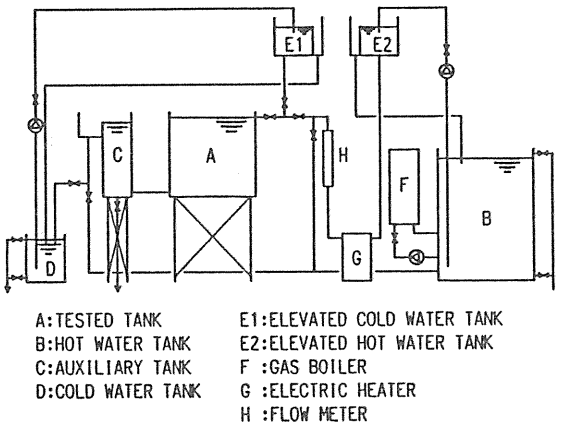

Fig. 15. Experimental installation for the temperature stratified tank.

Conditions

The effects of input conditions on the mixing process were examined by conducting experiments under the combination of various flow rates and various temperature differences between the inflow and the initial tank water. The flow rates and the temperature

differences covered a range from the realization of complete mixing to the forming of intense temperature stratification, as presented in Table 4 for example.

Table 4. Example of temperature and flow rate conditions*.

Case	Initial Temperature in the Tested Tank (°C)	Input Temperature (°C)	Flow Rate (L/min)	Ar_{in}
1	19.8	25.6	7.6	9.54×10^{-2}
2	19.6	29.0	7.8	1.56×10^{-1}
3	19.9	34.8	8.0	2.59×10^{-1}
4	19.9	44.5	7.9	5.64×10^{-1}
5	19.9	25.4	16.0	2.00×10^{-2}
6	21.0	31.3	15.8	4.42×10^{-2}
7	21.0	35.8	16.0	6.69×10^{-2}
8	21.0	45.9	15.7	1.33×10^{-1}
9	20.8	26.2	31.5	5.30×10^{-3}
10	20.4	31.3	32.2	1.12×10^{-2}
11	20.5	35.4	31.1	1.75×10^{-2}
12	21.2	46.2	31.0	3.45×10^{-2}
13	20.1	25.4	64.1	1.22
14	19.7	30.5	64.0	2.72
15	20.1	35.3	64.1	4.17
16	19.9	44.3	63.8	7.61

*Geometric conditions of the tested tank: Inlet position is center top, outlet position is center bottom, length of tank along direction of inflow is 0.8 m, width of tank perpendicular to inflow is 0.8 m, depth of tank is 0.8 m and diameter of inlet pipe is 45 mm (see Table 2).

The effects of geometric conditions on the mixing process were examined for various aspect ratios of the tank and the inlet and outlet shapes and their positions, as shown in Fig. 16. These conditions are listed in Table 5.

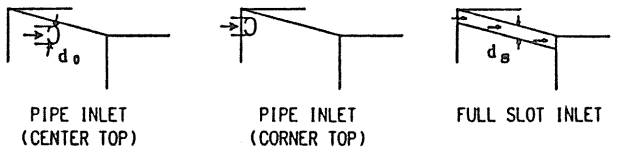

Fig. 16. Variations of the inlet type.

Table 5. Geometric conditions of tested tank.

Inlet Position	A : Center Top B : Corner Top	
Outlet Position	A : Center Bottom B : Corner Bottom C : Half Depth Center	
Length of Tank Along Direction to Inflow	0.2, 0.36, 0.4, 0.8 1.6	(m)
Width of Tank Perpendicular to Inflow	0.3, 0.4, 0.8	(m)
Depth of Tank	0.4, 0.8	(m)
Diameter of Inlet Pipe d_0	25, 45, 70	(mm)
Vertical width of Full Slot Inlet d_s	10, 15, 20, 25, 30, 35, 45, 50, 55, 70	(mm)

Identification of Model Parameter

Though it is usual to figure the outlet temperature as a representative response of the dynamic system, the temperature responses at three different levels near the tank bottom were regarded as the outlet response and were compared with model runs. This is because the temperatures in the outlet were not uniform, since the stratified layer is formed in the outlet when the layer reaches there.

From many experimental results, R_d in Eq. (10) could be regarded as the following constant value under all input conditions:

$$R_k = 0.4 \tag{12}$$

Fig. 17 shows the outlet temperature responses under a stepwise temperature input with various R_0 values. It is difficult to obtain a theoretical solution for Eq. (11) due to changing boundary conditions, so Eq. (11) was numerically worked out in finite difference form with time interval, t. The tank depth was divided into 400 sublayers for numerical

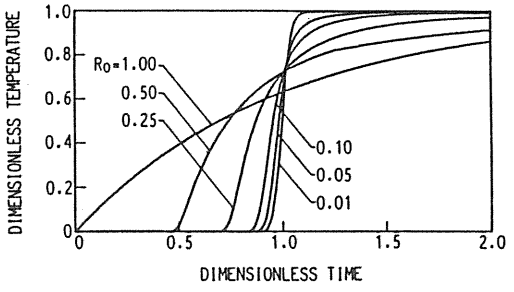

Fig. 17. Outlet temperature responses by the model under a stepwise temperature input with various R_0 values.

calculations. The number of sublayers in the complete mixing region was first calculated and then the temperature in this region was calculated from Eqs. (9) and (10) for each time step. Then temperatures of the sublayers in the piston flow region were calculated from Eq. (11) by the finite difference method using an upwind differencing technique. The boundary conditions were as mentioned above. If l becomes larger than the depth of the tank, the temperature in the tank is uniform and the piston flow region ceases to exist.

Each experimental response was compared with the calculated one, and the corresponding R_0 for experimental results was identified. Fig. 18 illustrates some example comparisons between the model runs and the experimental results at three different levels of the tank at central points near the bottom (40, 120, and 160 mm from the bottom [see Fig. 15]). The simulated output responses match the experimental responses well, except that a little difference occurs at later times due to heat loss at water surface. The error is quite negligible from the viewpoint of practical design.

For generalizing purposes, data were arranged using dimensionless numbers and plotted on a logarithmic scaled chart. The log-linear relations between l_0/d_0 or l_0/d_s and the inlet Archimedean number, Ar_{in}, derived from the input conditions, were obtained for each experiment, as shown in Fig. 19. It was experimentally proved that geometric conditions such as the horizontal positioning of the inlet and outlet and the aspect ratios of the tank have little effect upon the relations between l_0 and Ar_{in} on the whole. The relations for the pipe inlet and the full slot inlet are, however, presented differently. The reason that l_0/d_s of a slot inlet is relatively larger is attributed to larger input flow rate with the same Ar_{in}. It should be noted that l_0/d_0 or l_0/d_s will become constant at the extremely small Ar_{in}, due to constraint of the tank depth, and seem constant at the extreme right, due to the impossibility of identifying the scale of an extremely thin stratified layer. A minimum layer thickness may exist, as observed by Yoo et al.,[18] but that was not determined in this study because of the object of the study. Though Oppel et al.[19] pointed out the effect of Reynolds number defined by velocity inside the tank

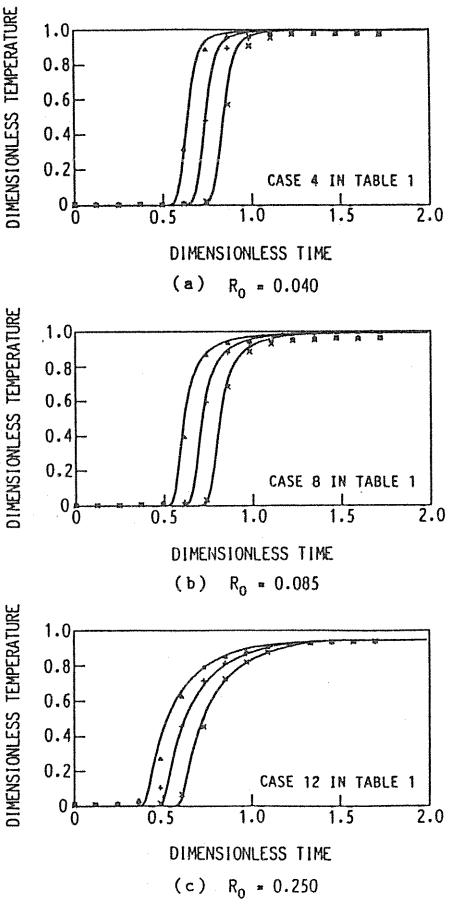

Fig. 18. Comparisons of the temperature responses between the model runs and the experimental results at three different levels of the tank at the central points near the bottom (40[×], 120[+] and 160[△] mm from the bottom), symbols are experimental results and solid lines are model runs.

and tank diameter on the mixing process, the variations of inside velocity didn't affect the relations of l_0 and Ar_{in} in our study. Oppel et al.[19] modeled the mixing process by using variable diffusivity, while diffusivities in the complete mixing region and the piston flow region were kept constant by the authors. This may be the reason that our results were not affected by the Reynolds number (or Peclet number) to an extent greater than the magnitude of experimental errors.

The regression equations of the linear portions are as follows:

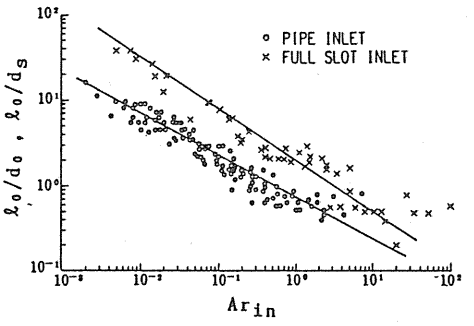

Fig. 19. Relations between the initial depth of complete mixing region, l_0, and the inlet Archimedean Number, Ar_{in}, for all experimental conditions.

1. The pipe inlet with diameter d_0

$$R_0 = l_0/L = 0.7 Ar_{in}^{-0.5} d_0/L \tag{13}$$

$$Ar_{in} = \frac{d_0 g(\Delta\rho/\rho_0)}{u^2} \tag{14}$$

2. The full slot inlet with vertical width d_s

$$R_0 = l_0/L = 2.0 Ar_{in}^{-0.6} d_s/L \tag{15}$$

$$Ar_{in} = \frac{d_s g(\Delta\rho/\rho_0)}{u^2} \tag{16}$$

Fig. 20 shows an example of calculated temperature profile results as compared to experimental results. The disagreement at early times is attributed to the assumption that the complete mixing region exists before the stratified layer formation. The calculated temperature profiles almost match the experimental profiles after the stratified layer formation. The little differences at the upper part of the tank may be attributed to heat

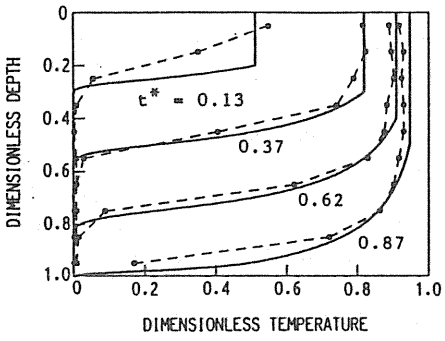

Fig. 20. Comparisons between predicted vertical temperature profiles and experimental results (case 7 in Table 1.) at times with progress of thermal charge, solid lines are the calculated profiles and broken lines are the experimental ones.

loss at water surface.

Extension to Variable Input Conditions

The following facts were observed in the experimental results under variable input conditions. In the case of flow rate reduction or input temperature rise, a new temperature-stratified layer is formed above the old one. In the case of flow rate increase or input temperature fall, the complete mixing region extends wider than the previous one. Therefore, temperature responses under variable input conditions must be estimated according to each situation.

R in Eq. (10) is recalculated as follows according to the change of Ar_{in}, which also makes it possible to apply simultaneous change of inflow rate and input temperature because both changes are expressed with the change of Ar_{in}.

1. In the case of Ar_{in} increase: u and $\Delta\rho$ in Eq. (14) or (16) take the new values immediately after the condition change. ρ_0 takes the value of the temperature in the complete mixing region at that time, because the new and shallow complete mixing region is formed above the old one. T^* is the time elapsed since the change.

2. In the case of Ar_{in} decrease: u and $\Delta\rho$ take the new values. ρ_0 takes the value used before the change, because the border of a new complete mixing region is formed below the old one. T^* is not renewed in this case. When the new input temperature is lower than that of the complete mixing region, dispersion due to gravitational force causes the temperature fall as well as an increase in the complete mixing zone, regardless of the new calculated R value. The dispersion naturally stops when the new temperature in the complete mixing region becomes higher than that below.

Fig. 21 compares the model runs with the experimental results. The mixing process for variable input conditions is not linear due to the existence of the temperature-stratified layer, so the estimations of temperature profile for these conditions are difficult. In this paper, inflow water after input condition change is assumed to mix completely in the new complete mixing region, but Fig. 21 shows little difference between estimated responses and experimental responses. These errors are considered negligible from the viewpoint of practical design. When low-temperature water enters from the bottom inlet, the calculation can be carried out by turning the model upside down.

Simultaneous inputs of high-temperature water from the top inlet and low-temperature water from the bottom inlet are encountered at simultaneous operations of both heat source and secondary side for actual HVAC systems having individual I/O style, as explained in Part 1. In this situation, three regions appear: the upper and lower complete mixing regions and the intermediate piston flow region with one-dimensional diffusion. The flow rate through the piston flow region was regarded as the difference of flow rates from the top and bottom inlets. The dimensionless time, T^*, was calculated from the flow rate difference. One complete mixing region increased and the other decreased according to T^*, but the minimum depths of the two complete mixing regions were assumed as their l_0's. If two complete mixing regions overlapped when large input condition change happened, the center of these calculated borders was regarded as new border. An example of a model run for an actual system having about 32 m^3 capacity water storage tank with the dimensions of 1.7×6.1×3.1 m and 100 mm pipe inlets is presented in Fig. 22. Input temperature and flow rates for the model calculation were given as measured input temperatures and flow rates that were smoothed for simple input conditions. On the whole, the simulated temperature profiles almost agree with measured profiles for a tank about 60 times larger than the tested tank, and the error is negligible, considering complicated variable input conditions.

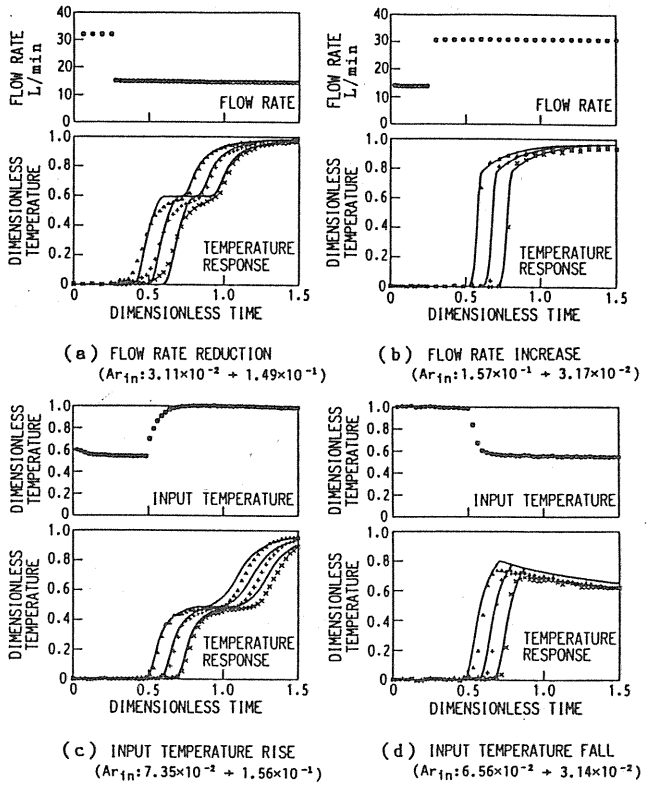

Fig. 21. Comparisons between predicted temperature responses and experimental ones at three different levels of the tank at the central points near the bottom (40[×], 120[+] and 160[△] mm from the bottom) under variable input conditions, symbols are experimental results and solid lines are model runs.

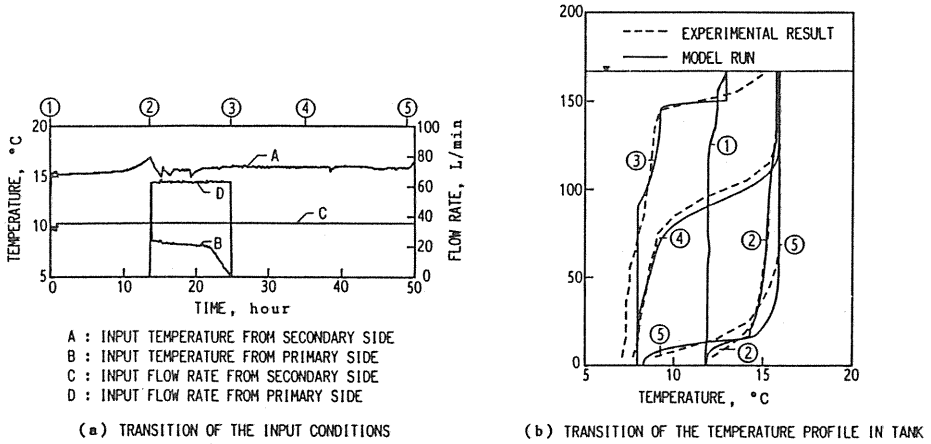

Fig. 22. Transitions of the input conditions and the temperature profiles in tank for an actual storage system under the condition of charge and discharge cycle, encircled numbers in (b) correspond to time indicated encircled numbers in (a).

3. System Simulation and Performance Estimation Tables

Storage efficiency is defined as the ratio of the actual storage or discharge of heat to the nominal storage or discharge of heat in the storage tank. The storage system is easily designed if the storage efficiencies are specified (see Part 1).

The storage efficiencies were calculated under various design conditions using a computerized operating simulation program in conformity with the experimental designs (Taguchi[13]; Cochran et al.[20]; Connor et al.[14]). The effect of each design condition on the storage efficiency was examined statistically, and estimation tables of the storage efficiency including the effects of significant design conditions were presented.

Computerized Operating Simulation

Storage efficiency under each set of design conditons was calculated by simulation using the following procedure. At first, simulation conditions were given for daily variation in the cooling or heating load, control methods for heat source (primary side) and HVAC (secondary side) systems, setup temperatures, heat source operation schedule, and the structure and composition of the tank. From daily load and heat source operation time, the required heat source output was derived and the initially assumed storage tank capacity was calculated. Then, the frist simulation was conducted, and the transition of the temperature profile in the tank was calculated. Two days of simulation wree enough to obtain the periodic steady state and to judge if the capacity was optimized according to the judgment based on the limit temperatures of both the primary and secondary sides. The capacity of the tank was modified and the simulation was conducted again until the tank capacity was optimized. The storage efficiency was then calculated from the equation defined in Part 1 using the final tank capacity and temperature profile after the convergence procedure. The procedure was the same as that for the multi-connected complete mixing storage tank in Part 1, except for dependence on a large-scale computer with the Fortran language.

It should be noted that heat loss from the tank wall was disregarded in the simulations. If the heat loss is taken into consideration in designs using the present results, the designers should follow the procedure explained in Part 1. The dead zone in the tank was also disregarded. The actual storage efficiency is given by multiplying the calculated storage efficiency by the ratio of the tank's dead zone to the full tank capacity.

Allocation of Factors to Orthogonal Array

The factors shown in Table 6 were selected as the design conditions that may affect the storage efficiency. The condition levels of each factor were given as the operating simulation conditions. Various setup temperatures and limit temperature difference ratios are presented schematically in Part 1. Peak R_0 in Table 6 is a parameter representing the performance of the temperature-stratified tank itself, which corresponds to the number of tanks for the multi-connected complete mixing type. The peak R_0 is defined as the larger value of a couple of R_0's, one of which is calculated from the peak load conditions for the secondary side and the other of which is for the design conditions for the primary side. The tank inlet sizes can be calculated from the peak R_0 by Eqs. (13) and (14) for the pipe inlet and Eqs. (15) and (16) for the full slot inlet if setup temperatures, flow rates, and tank depth are given.

The factors are allocated to the orthogonal array L-81 of the fractional factorial designs paying special attention to the interactions between factors as in Part 1, resulting

Table 6. Examined design conditions and their levels.

Design Conditions	Level 1	Level 2	Level 3
A : Heat Load Pattern for CWV Systems		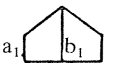	
B : Min./Max. Ratio of Daily Heat Load for CWV Systems, a_1/b_1 (CWV Min./Max.)	0.8	0.5	0.2
C : Heat Load Pattern for VWV Systems		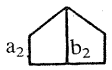	
D : Min./Max. Ratio of Daily Heat Load for VWV Systems, a_2/b_2 (VWV Min./Max.)	0.8	0.5	0.2
E : Daily CWV Heat Load Ratio to Daily Total Load (CWV Ratio)	0.2	0.5	0.8
F : Existence of Constant Delivery Control for CWV Systems (CDT)	No	Yes(1)*1	Yes(2)*2
G : Limit Temperature Difference Ratio for Primary Side (LTDR1)	0.4	0.6	0.8
H : Limit Temperature Difference Ratio for Heat Source	0.0	0.2	0.4
I : Limit Temperature Difference Ratio for HVAC Side (LTDR2)	0.2	0.4	0.6
J : Operation Schedule of Generator (Schedule)	0:00–24:00	7:00–22:00	22:00–8:00
K : Peak R_0	0.10	0.25	0.40
L : Temperature Difference Through the Coil at the Time of Peak Heat Load	5°C	10°C	15°C
M : Individual or Unified input/output*4 (I/O Style)	Individual	Unified	
N : Chilled or Heated Water Tank	Chilled	Heated	
O : Pipe or Full Slot Inlet	Pipe	Slot	

*1. Delivery temperature=design temperature of inlet water to coil

*2. Delivery temperature=design temperature of inlet water to coil $\pm$*3$0.2\times$(temperature difference through coil)

*3. positive for cooling, negative for heating

*4. individual input/output: unified input/output:

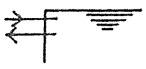

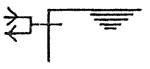

in three execution steps due to too many factors. The combination of condition levels is automatically decided by the orthogonal array. Simulation steps were classified as follows: The first and second steps included only variable flow rate systems (VWV), which make input conditions favorable for the performance of the storage tank. The third step included constant flow rate systems (CWV), or variable temperature difference systems (VTD), as well as VWV systems. There are normally three factorial levels, but factors with only two levels by nature were allocated by the dummy allocation method.

Analyses and Estimation Tables

In the first step, simulations including the effects of the eight factors (C, D, G, H, I, J, K and L) were executed with the individual input/output, the chilled water tank, and the pipe inlet, excluding factors related to the CWV systems. Examined by the ANOVA (analysis of variance), the limit temperature difference ratios for both primary and HVAC sides (G and I), the operation schedule of the generator (J), and the peak R_0 (K) were extracted as significant factors. The interaction between the limit temperature difference ratio for the primary side (G) and the peak R_0 (K) was also significant.

In the second step, the effects of three additional factors (M, N, and O) and those factors that proved significant in the first step were analyzed. The factors found to be insignificant were fixed at the second level in Table 6. Results of the second step ANOVA are shown in Table 7.

Table 7. Results of the second analysis of variance with significant factors.

Design Condition	Sum of Squares	Degree of Freedom	Mean Squares	F Distribution	Contribution (%)
G	0.523	2	0.262	95.4**	18.5
I	1.287	2	0.643	234.5**	45.7
J	0.323	2	0.161	58.8**	11.3
K	0.134	1	0.067	24.5**	4.6
M	0.055	2	0.055	19.9**	1.9
G×K	0.178	4	0.045	16.2**	6.0
I×K	0.065	4	0.016	5.9**	1.9
M×K	0.034	2	0.017	6.3**	1.0
M×J	0.044	2	0.022	8.1**	1.4
Error	0.162	59	0.003		7.7

Note. **: 1% of significance

Table 8. Results of the third analysis of variance with significant factors.

Design Condition	Sum of Squares	Degree of Freedom	Mean Squares	F Distribution	Contribution (%)
B	0.309	2	0.155	22.3**	6.3
F	0.603	2	0.301	43.4**	12.6
G	0.617	2	0.309	44.5**	12.9
I	2.020	2	1.010	145.5**	43.0
J	0.174	2	0.087	12.5**	3.4
K	0.093	2	0.047	6.7**	1.7
M	0.100	1	0.100	15.5**	2.0
B×E	0.082	4	0.023	2.9*	1.2
F×E	0.156	4	0.039	5.6**	2.8
F×I	0.076	4	0.019	2.7*	1.0
Error	0.340	49	0.006		12.2

Note. **: 1% of significance
*: 5% of significance

In the third step, the effects of the four factors (A, B, E, and F) related to the CWV systems, as well the significant factors in the second step, were analyzed. All insignificant factors in the first step were fixed at the second level. For the insignificant factors in the second step, the inlet was a pipe and the chilled water was stored. Table 8 shows the results obtained. The results of the third step were similar to the results of the multi-connected complete mixing tank in Part 1 except some factors.

Estimation tables of storage efficiency for the HVAC systems including only VWV systems and for the HVAC system including both VWV and CWV systems are presented in Tables 9 and 10. Most of the results are reasonable and easily understood. The storage efficiency becomes higher if the Min./Max. ratio of daily heat load for CWV systems is higher, the constant delivery is adopted, the limit temperature difference ratios for primary and HVAC sides are higher, the ratio of overlapped operating time of generator and HVAC sides to generator operating time is higher, the peak R_0 is smaller, and the unified input/output is adopted. Details of the effects of these factor are mentioned in Part 1 except for R_0. The interactive effect presented a minor complication explained below.

Table 9. Estimation table of the storage efficiency, η_s, for HVAC systems including only variable flow rate (VWV) systems.

Design Conditions		$\eta_s=0.981+\Sigma\Delta\eta_i$ Factorial Effects $\Delta\eta_i$			Condition Levels		
		Level 1	Level 2	Level 3	Level 1	Level 2	Level 3
G : LTDR1		−0.095	−0.006	0.101	0.4	0.6	0.8
I : LTDR2		−0.156	0.003	0.153	0.2	0.4	0.6
J : Schedule		0.012	0.071	−0.082	0–24	7–22	22–8
K : Peak R_0		0.034	0.023	−0.057	0.10	0.25	0.40
M : I/O Style		−0.018	0.037		Individual	Unified	
G×K: LTDR1 ×Peak R_0		K1	K2	K3			
	G1	0.027	−0.046	0.019			
	G2	0.057	−0.016	−0.045			
	G3	−0.084	0.062	0.022			
I×K: LTDR2 ×Peak R_0		K1	K2	K3			
	I1	0.019	−0.038	0.019			
	I2	0.014	0.031	−0.045			
	I3	−0.033	0.007	0.026			
M×K: I/U Input ×Peak R_0		K1	K2	K3			
	M1	0.018	−0.001	−0.017			
	M2	−0.037	0.002	0.034			
M×J: I/U Input ×Schedule		J1	J2	J3			
	M1	−0.003	−0.019	0.022			
	M2	0.006	0.037	−0.043			

Note. Confidence interval for mean value=±0.053 at the 0.05 level

Table 10. Estimation table of the storage efficiency, η_s, for HVAC systems including both variable flow rate (VWV) systems and constant flow rate (CWV) systems.

Design Conditions		$\eta_s=0.967+\Sigma\Delta\eta_i$ Factorial Effects $\Delta\eta_i$			Condition Levels		
		Level 1	Level 2	Level 3	Level 1	Level 2	Level 3
B : CWV Min./Max.		0.072	0.007	−0.079	0.8	0.5	0.2
F : CDT		−0.106	0.001	0.105	No	Yes(1)	Yes(2)
G : LTDR1		−0.104	−0.006	0.110	0.4	0.6	0.8
I : LTDR2		−0.201	0.017	0.184	0.2	0.4	0.6
J : Schedule		−0.023	0.064	−0.042	0–24	7–22	22–8
K : Peak R_0		0.036	0.010	−0.050	0.10	0.25	0.40
M : I/O Style		−0.025	0.050		Individual	Unified	
B×E: CWV Min./Max. ×CWV Ratio		E1	E2	E3			
	B1	0.044	0.002	−0.046			
	B2	0.004	−0.028	0.024			
	B3	−0.049	0.027	0.022			
F×E: CDT ×CWV Ratio		E1	E2	E3			
	F1	0.062	0.002	−0.065			
	F2	−0.007	−0.043	0.049			
	F3	−0.049	0.040	0.015			
F×I: CDT ×LTDR2		I1	I2	I3			
	F1	0.039	0.009	−0.048			
	F2	−0.026	0.023	0.004			
	F3	−0.013	−0.032	0.045			

Note. Confidence interval for mean value=±0.092 at the 0.05 level

The interaction between the limit temperature difference ratio and the peak R_0 (G×K and I×K) was significant, as the advantages of high limit temperature difference ratios are often lessened by favorable small peak R_0, as shown in Fig. 23. The interaction

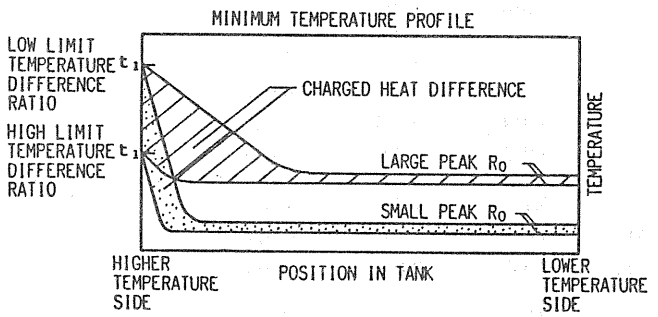

Fig. 23. Ralation between the difference of temperature profiles at the end of cold water charging and the interaction of the limit temperature difference ratio for primary side and the peak R_0 is larger than that under small peak R_0.

between the individual or unified input/output and the operation schedule of the generator (M×J) was also significant, as the effect of the unified input/output is strengthened by overlapping the htermal charge and discharge. The interaction between the individual or unified input/output and the peak R_0 (M×K) proved to be significant as well due to reasons similar to the interaction between the limit temperature difference ratio and the peak R_0. This is because the unified input/output has effects similar to the high limit temperature difference ratio. The significant interactions in the third step (B×E, F×E and F×I) were significant for the multi-connected complete mixing tank as well (see Part 1).

Part 3. Estimation of Storage Performance and Application Results of Self-Balanced Temperature-Stratified Tank

1. Principle

The temperature stratification effect is fundamentally realized by maintaining high temperature difference between inflow water and that inside the tank while maintaining low inlet velocity. This resulted in a large Archimedean number at the inlet, which dominated the characteristics of the flow field due to the existence of buoyancy. However, such a favorable situation is not realized in many actual HVAC systems. The typical unfavorable situation appears when a three-way valve control at the cooling/heating coil is used.

The authors thought of utilizing the natural force of the incoming water to discriminate the inflow position by means of natural circulation or thermosyphon between the main tank and small-sized subheader tanks.

The principle described here clearly shows that a low-temperature water flow into the subheader naturally falls down the header and flows into the main tank through the appropriate connecting pipes and vice versa.

Fig. 24 shows the principle of self-balancing. Actual volume of the subheader

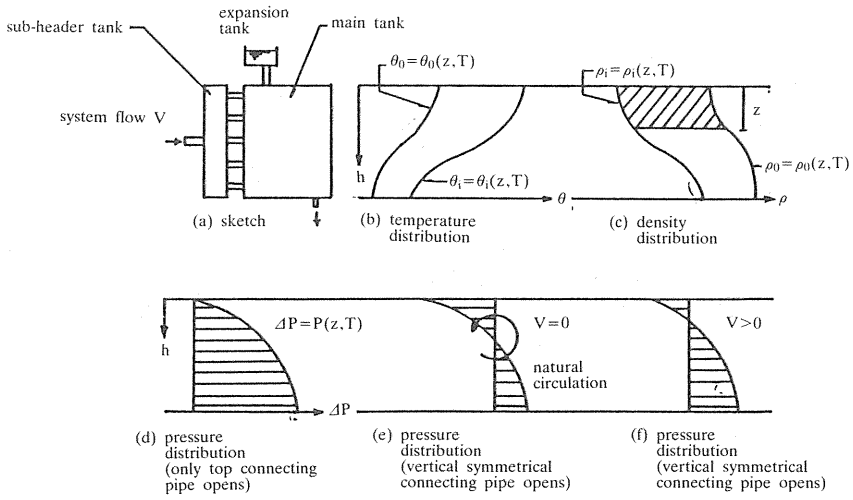

Fig. 24. Principle of self-balanced temperature stratified tank.

tank is far less than 1.0% of the main tank. The temperature and density distribution at time t are represented in (b) and (c). The results of the pressure difference between the two tanks are shown in (d), which produce a natural circulation between the tanks if all of the connecting pipes are open and pressure distribution reaches that of (e) or (f). When the system flow, $F_{o,in}$, exists, the pressure difference, $\Delta P(z,T)$, at depth z and time T is

$$\Delta P(z,T)=\int_0^z\{\rho_0(z,T)-\rho_i(z,T)\}g\,dz+P_s \tag{17}$$

where $\rho_0(z,T)$ and $\rho_i(z,T)$ represent water density in the subheader tank and main tank at depth z and time T, respectively. P_s is static pressure at the top of the subheader tank tank, which is decided by flow balance between the main tank and the subheader tank, as shown in Fig. 1, and g is gravity acceleration. This pressure difference is assumed to be equal to the pressure drop, ΔP_{L_j}, at connecting pipe j.

$$\Delta P_{L_j}=\zeta_j\frac{\rho_{con_j}}{2}u^2_{con_j}=\Delta P(z_j,T) \tag{18}$$

where u_{conj} is the velocity in the connecting pipe j, ρ_{conj} is the water density in the connecting pipe j, which is equal to that of the water at the same level in the upstream tank, and z_j is the vertical distance from water surface to the connecting pipe j.

The coefficient of resistance, ζ, is expressed as

$$\zeta_j=\zeta_1+\lambda\frac{l_{con_j}}{d_{con_j}}+\zeta_2 \tag{19}$$

where l_{conj} is the length of connecting pipe, ζ_1 is the resistance coefficient at the pipe inlet, ζ_2 is the pipe outlet resistance, and λ is friction loss coefficient. $\zeta_1+\zeta_2$ is nearly 1.5, and λ is approximated as

$$\begin{aligned}&\lambda=64/Re, \text{ for laminar flow}\\&=0.04, \text{ for transition boundary}\\&=0.055\{1+(4+10^6/Re)^{1/3}\}, \text{ for turbalent flow.}\end{aligned} \tag{20}$$

The second term in the right side of Eq. (19), which is the friction loss of the connecting pipe, may be neglected, because of the short pipe length.

The flow rates at the connecting pipes are estimated by equating the algebraic sum of the flow rates to and from the main tank with $F_{o,in}$, as follows.

$$F_{o,in}=\sum_j A_{con_j}\cdot u_{con_j}=\sum_j A_{con_j}\sqrt{\frac{2}{\zeta_j\rho_{con_j}}\Delta P_{L_j}} \tag{21}$$

where A_{conj} is the area of each connecting pipe j. The product of u_{conj} and A_{conj} shows the flow rate in the connecting pipe j, which shall be called "connect flow" hereafter.

Furthermore, the flow in the region of each tank divided by connecting pipes and/or the system inflow pipe shall be called "in-tank flow" hereafter. The flow rates and directions are not constant and are decided by mass balance equations consisting of system flow, in-tank flow, and connect flow between the main tank and subheaders. Actually, the in-tank flow dominates the temperaures profile of each tank.

2. Mixing Model

The mixing model is as follows

1. Mixing at the top and bottom inlet: "Buoyant inflow" results in the combination model in which a portion of the complete mixing region, l_m, appears near the boundary surface at the top and the bottom with or without a neighboring piston flow region with one-dimensional downstream diffusion. See Fig. 25 and refer to Part 2. When the mixing length is too large, the piston flow region disappears. "Buoyant inflow"

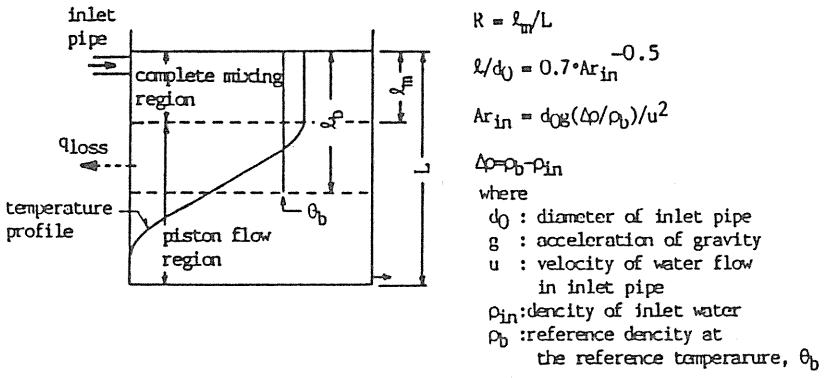

Fig. 25. Modeling of thermal process in tank based on R-model.

is defined as higher temperaure water input at the top, or lower temperature water input at the bottom, than the water temperature at the corresponding position of the tank as a receiver. The R-model described in Part 2 has been slightly changed in order to simulate actual situations. The reference temperature in the tank for calculating the Archimedean number is assumed as the mean temperature of water in twice the mixing length, l_m. This length was suggested by the fact that complete mixing resulted when the initial R-value, R_0, was nearly 0.5 at the time of initial inflow into a tank with a uniform temperature. Therefore, it is considered that approximately twice the length of the downward at the opposite wall occurs during the beginning of the inflow. Thus, the density corresponding to the mean temperature in this length, $2l_m$, was assumed to affect the buoyancy of the inflow jet at a higher temperature. This situation was supposed to exist even in the transient condition and was verified by comparison between simulations and experiments (Kawabata et al.[21]; Nakahara et al.[22]). The visualization also showed that, even after the initial inflow, the downward inrush at the opposite wall was present down to

approximately twice the length of the complete mixing region presumed by the temperature measurements. This modification allows practical application of the R-model to any kind of initial condition and vertical temperature distribution in existence, and it will be called the practical R-model, hereafter. With this procedure, the mixing zone increment according to the progress of charging, which was described in Part 2, is automatically introduced. The model is described a follows;

Complete mixing region:

$$\frac{d\theta}{dT}=\frac{Q}{V\cdot R}(\theta_{in}-\theta)+\frac{q_{loss}}{V} \tag{22}$$

$$R=l_m/\mathrm{L} \tag{23}$$

$$l_m/d_0=0.7\cdot Ar_{in}^{-0.50} \tag{24}$$

$$Ar_{in}=d_0\cdot g\cdot(\Delta\rho/\rho_b)/\mathrm{u}^2,\quad \Delta\rho=\rho_-\rho_{in} \tag{25}$$

Piston flow region:

$$\frac{\partial\theta}{\partial T}=\varkappa\frac{\partial^2\theta}{\partial z^2}-U\frac{\partial\theta}{\partial z}+\frac{q_{loss}}{3600\cdot V} \tag{26}$$

where V, L, and l_m are the tank volume, tank depth, and mixing length, respectively, and u, Q, Q_{in}, and ρ_{in} are the velocity, flow rate, temperature, and density of water flow introduced from the pipe inlet of which the diameter is d_0. The θ is the temperature of the complete mixing region or of the piston flow region, and ρ_b is the density of the tank water at the reference temperature in the tank for calculating the Archimedean number, Ar_{in}. The q_{loss} is the heat loss/gain through the tank wall, estimated by the temperature difference between the water in the tank and ambient, as described in Part 1. Volumetric specific heat, $c\rho$, was assumed to be unity as the unit of volume and heat are described in m^3 and Mcal, respectively. The $\varkappa$ is thermal diffusivity, U is vertical velocity in the piston flow region of the tank, and z is the depth from water surface in Eq. (26).

The "mixing inflow," which corresponds to a condition contrary to that of the buoyant inflow, completely and instantaneously mixes with the water under or above the input and ceases to mix when the water temperature of the mixed region becomes the same as the neighboring water under or above it. The remaining part of the section is pushed out as piston flow with one-dimensional diffusion. Almost no horizontal temperature variation was observed by the experiments.

2. Mixing at the intermediate inlets: The inflow at the intermediate position is always a mixing inflow as described in section 1, above, except that the temperaures of both the inlfow water and the tank are exactly the same. The method of calculation is the same as the mixing inflow described above. The heat either diffuses upward or downward.

3. Model Validation

The simulation algorithm of the mixing model, including the principle of self-balancing described above, was validated by comparing the calculated results with experimental results under various conditions. Fig. 26 shows the details of the experimental model. (The experimental system is the same as described in Part 2.) The number of connecting pipes was fixed as three. The validation was conducted under the step input. The topics chosen here are the validity of the model itself and the treatment for reference temperature for calculating Archimedean number and friction loss through the connecting pipe.

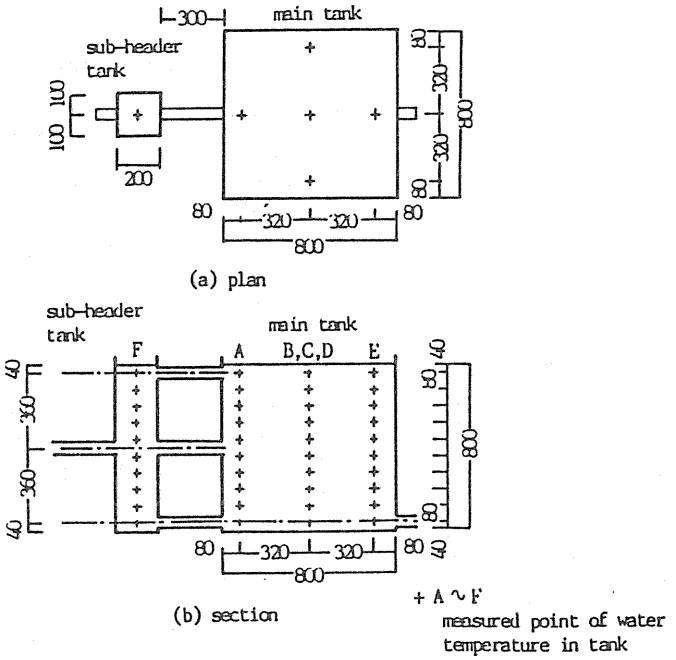

Fig. 26. Experimental model of self-balanced temperature stratified tank.

Validity of Model

Fig. 27(a) shows a comparison of the temperature profile in the tank and the outlet temperature response among the experimental results and calculation results with or without the R-model described in Eqs. (22)–(25). The one without the R-model, which shall be called the G-model hereafter, treats the entire tank as a piston flow region with one-dimensional diffusion. Results of calculations using the R-model agree better with experimental ones than those of the G-model, and the results from the G-model show a stronger stratification as a result of neglecting the mixing effect. However, the predicted temperature profile in the tank still does not fit the experimental one, especially at an early time, due to the following reasons. One is that the R-model uses the imaginary

perfect mixing length, l_0, as an initial value of l_m, which was derived from regression analysis between Ar_{in} and l_0, so that the computed response does not fit at an early stage.

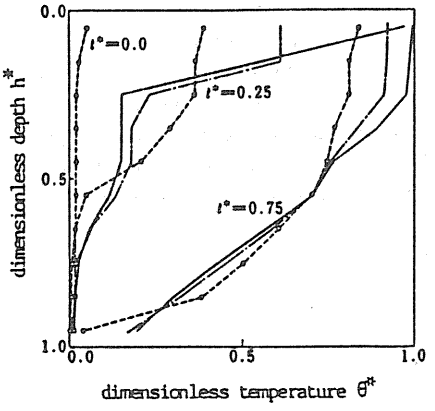

temperature profile in tank

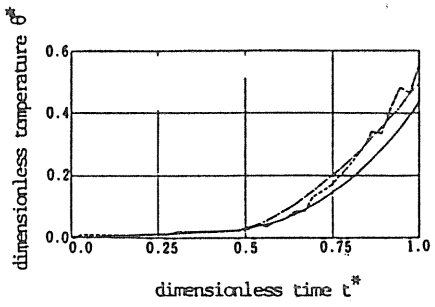

Condition: Flow rate through the system into the tank, is 14.5ℓ/min and temperature difference between inlet water and initially uniform tank water, Δt, is 9.6

(a)Comparison between R-model and G-model

explanatory note:
—·—practical R-model ——G-model
------experiment

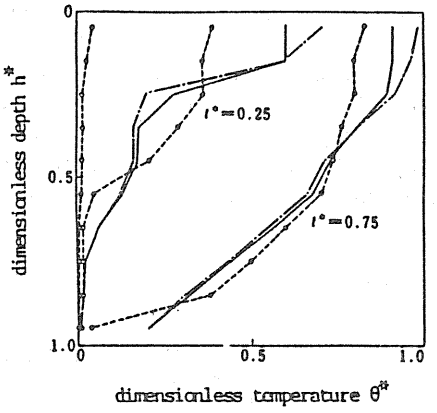

Condition: Flow rate through the system into the tank, $F_{o,in}$, is 14.5ℓ/min and temperature difference between inlet water and initially uniform tank water, Δt, is 9.6

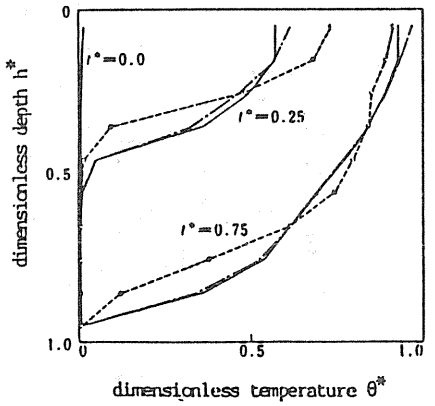

Condition: Flow rate through the system into the tank, $F_{o,in}$, is 7.4ℓ/min and temperature difference between inlet water and initially uniform tank water, Δt, is 19.8

(b)Comparison between three alternatives for reference water temperature

explanatory note:
——mean temperature in twice the mixing length, Θ_b, as the reference temperature (practical R-model)
—·—temperature at bottom of tank, Θ_{bot}, as the reference temperature
-----experiment

Fig. 27. Model validation.

Another reason is that static pressure, P_s, which is caused by system flow, was assumed in Eq. (17) to be the same value for each connecting pipe, while the force of inertia actually affects the connecting pipe located at the same vertical position with the system inflow. This results in too much flow predicted through the upper connecting pipe, which causes a predicted temperature higher than that in the experiment. Further studies are needed on these aspects. Also, the outlet temperature of the experimental result sometimes shows unique drops and rises (e.g., at $T^*=0.87$). This behavior is considered to be caused by discontinuous extention of the complete mixing region. This can be predicted by the concept of the practical R-model, although the response does not coincide with the experiment. However, it will be modified with more precise identification of the length of the complete mixing region, l_b. However, this degree of difference does not have a grave effect on predicting the storage performance.

Reference Water Temperature for Calculating Ar_{in}

Fig. 27(b) shows the comparison of the temperature profile on the tank among the experimental results, calculated results with the practical R-model, and another concept of applying the R-model. As mentioned before, the practical R-model adopts the mean temperature of water in twice the mixing depth as the reference temperature for calculating the Archimedean number, Ar_{in}. Another application uses the outlet temperature as the reference temperature, as it has a similar effect of extending the mixing length, l_m. The practical R-model can be used for the prediction of thermal characteristics with almost the same accuracy as the original one. Fig. 27(a) shows that the outlet temperature response to step input can be predicted with sufficient accuracy for practical use by the original R-model. Further, some improvement can be recognized on the temperature profile in the upper part of the tank by use of practical R-model. Therefore, the practical R-model is assumed to be applicable to any existing temperature profile in the tank with sufficient accuracy, not only to the step input.

Neglect of Connecting Pipe Friction

The friction loss through the short connecting pipe may be negligibly small compared to that at the inlet/outlet. Fig. 28(a) shows the results of calculation with and without the former friction loss, validating its neglect.

4. Characterisitcs of Balanced Storage

Several basic characteristics were investigated through numerical simulation and experiment. Numerical simulation using the above-mentioned algorithm was considered validated by comparisons in Fig. 27 and Fig. 28(a). The explicit finite difference method suffers from restrictions concerning the time interval necessary for the calculation to maintain stability, which affects the accuracy of the calculation. As the magnitude of diffusion is negligible compared to the speed of advection of water flow in actual operation, the stability of Eq. (25) is assured in the advancing scheme if the non-dimensional time interval, ΔT^*, satisfies

$$\Delta T^* < \Delta z^*$$

$$\Delta T^* = F_{o,in}\,\Delta T/\mathrm{V},\quad \Delta z^* = \Delta z/L \tag{27}$$

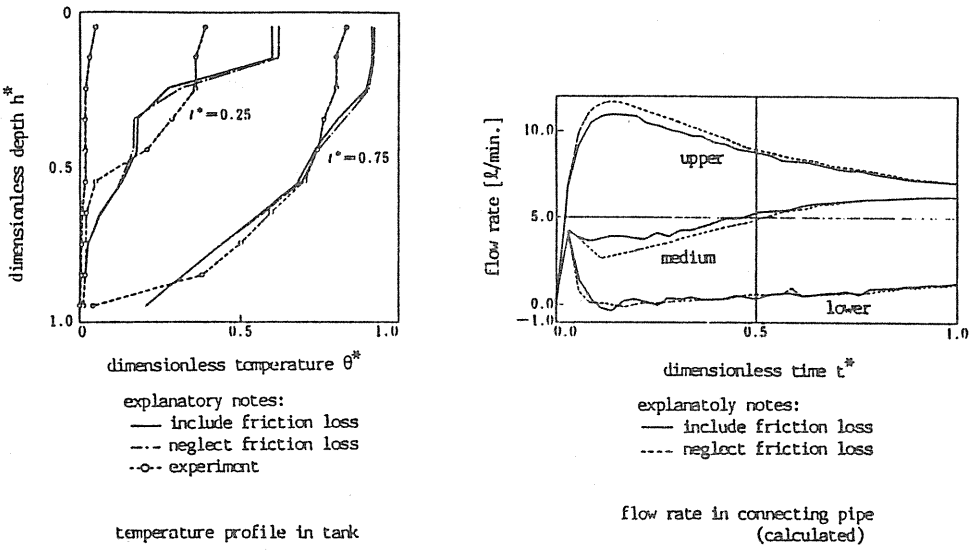

(a)Friction loss at connecting pipe

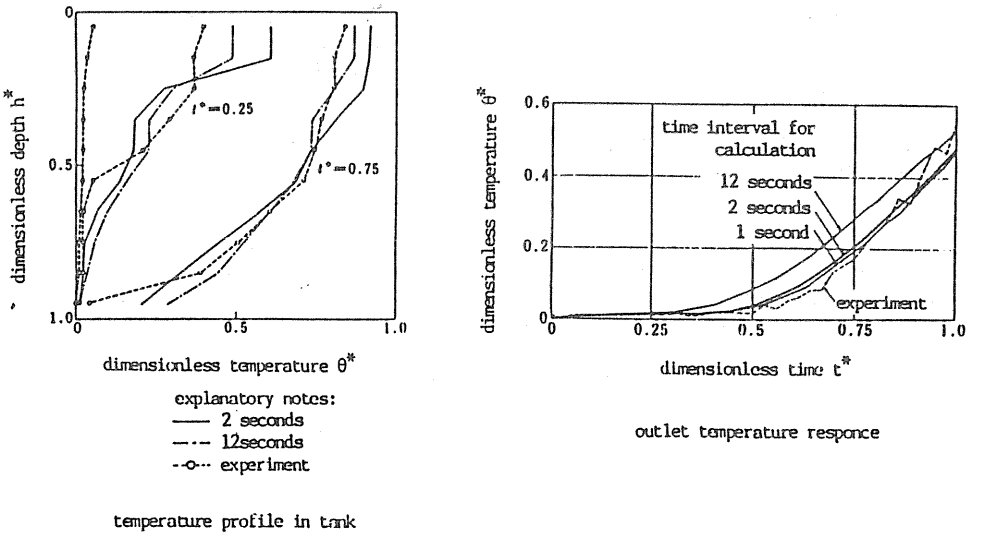

(b)Time interval for calculation

Fig. 28. Validation of simplified process.

where ΔT is time increment in real time, and Δz and Δz^* are spatial steps in real distance and dimensionless distance, respectively. Reduction of the computation time can be achieved by large ΔT and large Δz, but it is offset by reduction of the accuracy, as shwon in Fig. 28(b). As shown in the figure, the calculated result of outlet temperature

response at a 12-second increment rises considerably faster than the experimental one, but a 2-second increment is enough to achieve good agreement. This corresponds to $\Delta z^* = \Delta T^* = 1/67$. The following figures were calculated using this time interval.

Tank Height

As the effect of self-balancing depends on the natural circulation force between the main tank and each subheader expressed by the integral in Eq. (17), the height of the tank should affect the degree of stratification. Therefore, the Archimedean number based on the tank height as the representive length, that is,

$$Ar_h = \frac{g \cdot \Delta \rho \cdot L}{\rho \cdot u^2} \tag{28}$$

was assumed to be a reasonable parameter expressing the characteristics of the self-balanced tank. Fig. 29 shows the calculated results of the temperature profile in the main tank and the outlet temperature response under the condition shown in the figure. As is clear from the figure, the results with same Ar_h are almost the same and the assumption above mentioned is validated.

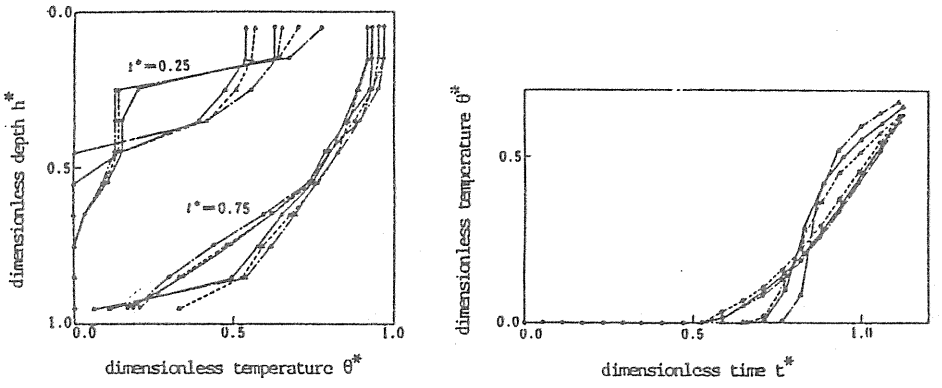

explanatory notes and conditions:

●——● tank height is 80cm, input temperature is 24.6°C, Ar_{in} is 7.24×10^{-2} and Ar_h is 1.16

●- - -● tank height is 120cm, input temperature is 23.2°C, Ar_{in} is 4.82×10^{-2} and Ar_h is 1.16

●—·—● tank height is 200cm, input temperature is 22.0°C, Ar_{in} is 2.89×10^{-2} and Ar_h is 1.16

△——△ tank height is 80cm, input temperature is 59.6°C, Ar_{in} is 7.10×10^{-1} and Ar_h is 11.36

△- - -△ tank height is 120cm, input temperature is 51.5°C, Ar_{in} is 4.73×10^{-1} and Ar_h is 11.36

△—·—△ tank height is 200cm, input temperature is 35.0°C, Ar_{in} is 2.84×10^{-1} and Ar_h is 11.36

common conditions: 10ℓ/min.; flow rate, 20°C; initial temperature in tank

Fig. 29. Effect of tank height.

Capacity of Subheader

An excessively large capacity of the subheader will weaken the self-balancing effect due to the mixing therein, but the effect on the temperature profile is not so sensitive, as shown in Fig. 30, provided the volume of the subheader is less than a tenth of the main tank.

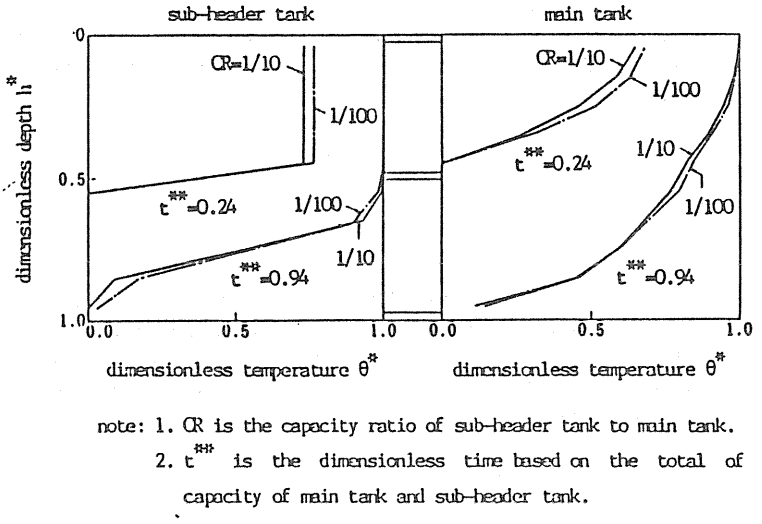

Fig. 30. Effect of the variation in capacity of subheader tank.

Number and Position of Connecting Pipes

The effect of the number and position of connecting pipes on the mixing process in the main tank was examined experimentally. The tank examined was a cylindrical one installed in an actual solar system for research and development on optimal control of solar system.[23] The tank was 1.5 m in height. The main tank was 0.8 m in diameter and the subheader was 0.2 m in diameter, resulting in a capacity ratio of the latter to the former of 0.0625. Both tanks are connected at five points, and each connecting pipe can be opened or closed independently for convenience. Water is drawn from the bottom of the tank and heated by the electric heater and returned into the middle part of the subheader tank. Charging with heated water was performed under constant flow rate and variable temperature in a sequential ramp mode, as shown in Fig. 31. The initial temperature profile in the tank was set in a stratified condition in each experiment, as shown at time 0 profile in Fig. 31.

Fig. 31 shows the differences among the temperature profiles with different numbers and positions of the connecting pipes. In the following discussion, it is assumed that the highest value of the initial temperature in the tank is sufficient to be used in a secondary heating circuit. It is also assumed that the water temperature at the bottom must be maintained for cooling as far as possible, so it can be assumed that the smaller the variation of temperature at top and bottom, the better the performance of the tank. The performance at one point input (ST-1) is considered the same as the original nonbalanced

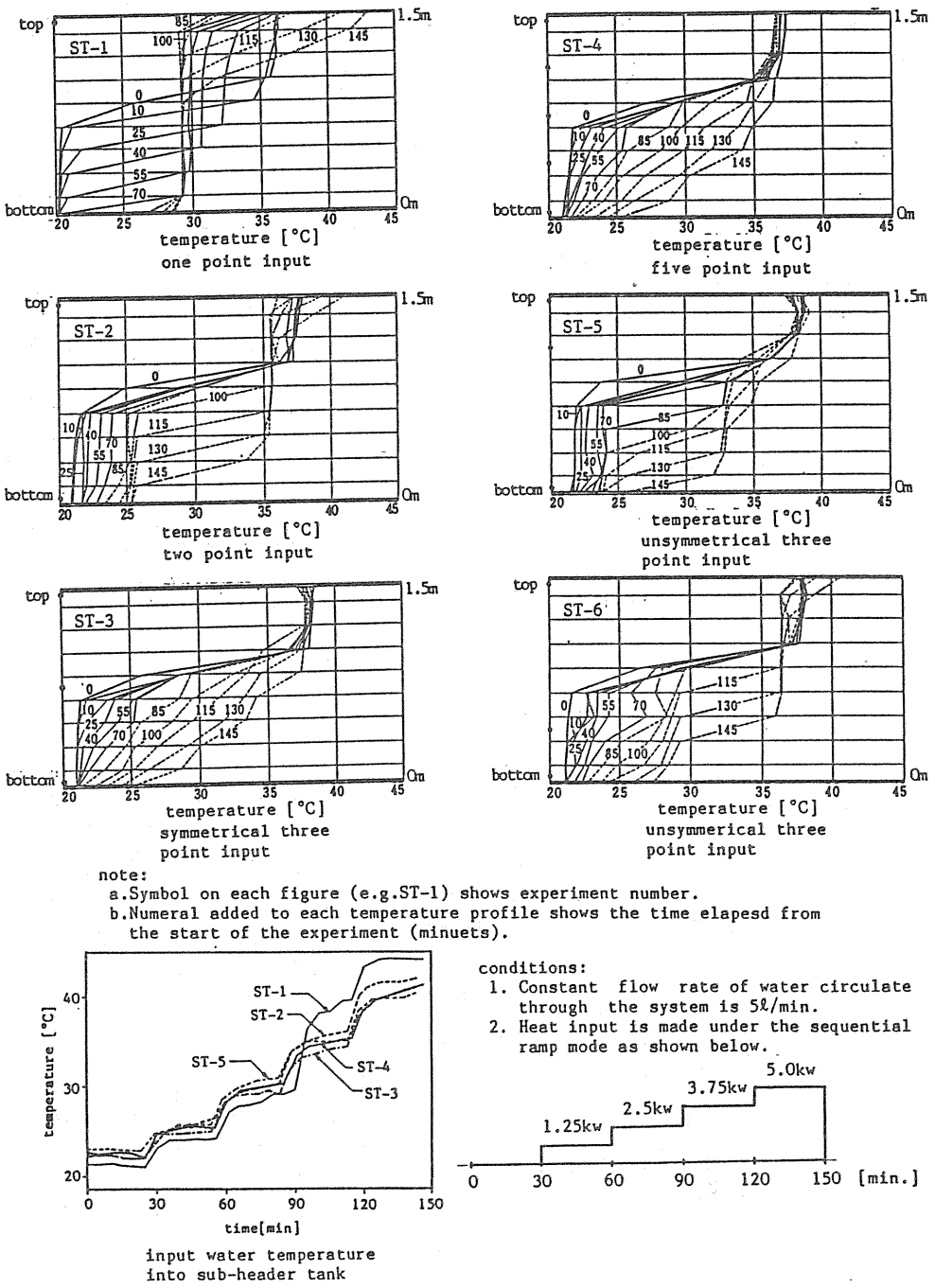

Fig. 31. Effect of number and position of connecting pipe (experimental results).

temperature-stratified tank, as reported in Part 2. The stratification rapidly decays just after the low temperature input. Comparing figures with each other, the following information can be acquired.

1. In the case of two-point input (ST-2), thermal performance of the tank is improved relatively compared with the case of one-point input, but strong mixing with an accompanying temerature rise in the lower side under the initial low temperature input still remains. Thus the outlet temperature rises and overheated water is introduced into the subheader and the temperature at the top of the tank rises excessively.

2. Three-point input (ST-3) prevents the mixing observed in the case of two-point input and maintains almost constant temperature both at the top and the bottom of the tank, because the intermediate inlet contributes the effective charge of intermediate temperature input to the middle part of the tank.

3. Five-point input (ST-4) shows almost the same characteristics as the three-point charge.

4. Unsymmetrical three-point input in which an intermediate input deflects to the upper part (ST-5) causes mixing similar to that of the two-point input at the lower part of the tank, but it prevents mixing at the upper side in the tank after the input temperature becomes relatively high, because the intermediate inlet starts to play a role in self-balancing after the temperature of the input water becomes high. A contrary phenomenon is observed in the case of deflecting intermediate input to the lower part (ST-6).

Thus, three symmetrically allocated inlets seem to be reasonable for arbitrary temperature inputs from the viewpoint of economy as well as the principle of self-balancing.

5. System Simulation

The air-conditioning system shown in Fig. 32, which is almost similar to that introduced in Part 1, was composed as the prototype, including the self-balanced

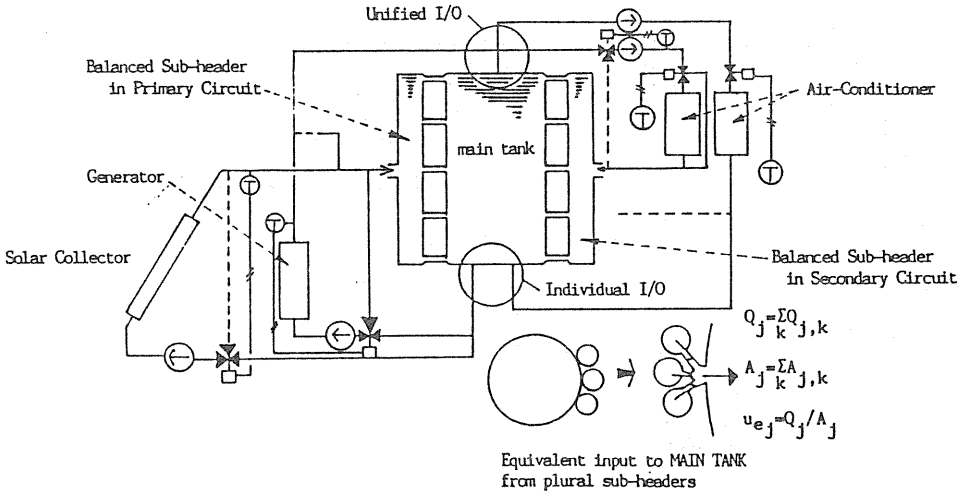

Fig. 32. Eomposition of HVAC and energy system including self-balanced water thermal storage tank.

thermal storage system. Simplified system descriptions and simulation conditions are as follows.

1. The subheader in the secondary circuit (air-handling unit side) can be divided into two: a VWV system and CWV system, or a system with a large temperature difference and a system with a small temperature difference.

2. The subheader on the primary circuit (cool/heat generator side) can either be attached or not. Conclusively, the constantly controlled temperature input should be directly returned to the main tank with a sufficiently large Archimedean number, but variable temperature input, such as the outlet from solar collectors, which has no outlet temperature control, or small Archimedean number input more than 0.1 in R-value, should be introduced via the subheader.

3. Heat generator (chiller, heat pump, or heat exchanger) should be equipped with an outlet temperature control using a three-way valve at the suction side in order to maintain a satisfactory delivery temperature to the air-handling unit.

4. Controls for the cooling/heating coil in the air conditioner were either a two-way valve, three-way valve, or no control valve, which correspond to VWV, the favorable side of a variable temperature system for the two-way valve, and CWV, the unfavorable side of a variable temperature system for the other two.

5. Constant temperature delivery control (CDT) can be used to offset the disadvantage of the CWV system (see Part 1).

6. The style of the inlet/outlet, individual or unified, will affect the storage efficiency due to the decreasing effect of the mixing range, as well as the raising effect of the limit temperature of the secondary circuit, as described in Part 1.

7. The mixing model for plural inputs from more than two subheaders has not been established, so all the inputs from subheaders at the same level, j, are synthesized into one, which has the equivalent input conditions of diameter, d_{e_j}, velocity u_{e_j}, as

$$d_{e_j}=\sqrt{\sum_k d_{con_{j,k}}^2} \tag{29}$$

$$u_{e_j}=\sum_k Q_{j,k}/(\pi d_{ej}^2/4) \tag{30}$$

where $d_{con_{j,k}}$ and $Q_{j,k}$ are the diameter and the flow rate from j th connecting pipe of k th subheader, respectively. This assumption is not unrealistic if strict similarities are required.

8. Due to constraints from using microcomputers, the saving of computing time was attemped as follows:

a) Computing time interval ΔT was varied according to each in-tank flow at the section of the tank under computation. The maximum ΔT was decided as the smaller value of either $\Delta z/U$ or $l_m/5U$. The former assures stability of the piston flow zone, and the latter was assumed as the allowable limit value to approximate the temperature change of the complete mixing zone.

b) Subheaders are critical in computation time because of very large water change rates, so that the size of the subheader was assumed to be unrealistically large as compared to actual application, shown in a later chapter, but not large enough to have more than one-tenth the capacity of the main tank, which has little effect on the temperature profile (see Fig. 30).

c) If a vertical inversion of temperature occures at any position in any tank, it is assumed that diffusion due to gravity/buoyancy instantaneously eliminates it at the end of each computation time interval.

Refer to Part 1 for the system simulation program. Computation time for 24 hours ranges from 30 minutes to 3 hours with the case changes, and twice the time is required to attain the steady state in two days. When acquiring optimal volume based on the limit temperature (see Part 1), two to five times more computation time for two days is necessary.

6. Estimation of Storage Efficiency

In order to examine the significant factors affecting the storage performance, system simulations were conducted under the combination of factors allocated with the orthogonal array by design of experiment. The details of this method were described in Part 1. The factors consist of some of those described above in "Characteristics of Balanced Storage" and some of those adopted commonly in both Part 1 and Part 2 as shown in Table 11.

Table 11. Factors and levels for design of experiment.

	Non-Balanced	Balanced	1	2
A	Type of Connection	Number of Subheaders in Secondary Circuit	slit / pipe	2 / 1
B	I/O Style	Existance of Subheader in Primary Circuit	unified / individual	None / Exist
C	Number of Tanks	Number of Connecting pipes	5 / 1 tanks	3 / 7 pcs
D	Existence of Constant Delivery Temperature Control for CWV System (CDT)		Exist	None
E	Daily CWV Heat Load Ratio to Daily Total Heat Load (CWV Ratio)		0.2	0.8
F	Coil Temperature Difference for CWV System		10	5°C
G	Tank Depth		10	5 m
H	Limit Temperature Difference Ratio for VWV System of HVAC Side (LTDR2)		0.4	0.2
I	Initial R-Value		0.1	0.4
J	Operation Schedule of Generator (Schedule)		0–24	22–8
K		I/O Style	—	Unified / Individual

The former group consists of the number of subheaders, both on the primary circuit and the secondary circuit, and the number of connecting pipes, while those belonging to the latter are the existance of constant delivery temperature control for a CWV system (CDT), the daily CWV heat load ratio to the daily total heat load (CWV Ratio), and the limit temperature difference ratio of the delivered chilled water for VWV system (LDTR2), or hot water to air-handling unit, and remaining factors in Table 11. Those latter three were already proved quite significant either in multi-connected complete

mixing tanks and single, nonbalanced stratified tanks as presented in Part 1 and Part 2, respectively. For saving computing time and placing emphasis on examining the significance of effects rather than estimation, $L_{32}(2^{31})$ orthogonal table was adopted. In order to compare the characteristics with a simple temperature-stratified (nonbalanced) storage tank, experiments of the same scale were conducted for the nonbalanced type as shown in Table 11. The first group of factors described above was replaced with those exhibiting the characteristics of multi-connected temperature-stratified tanks.

Unlike the preceding two papers, the limit temperature difference ratio for a CWV system, which was a significant factor in the preceding two prototypes, was replaced by the actual temperature difference value, assuming the use of the fan coil unit system with low temperature difference, because it should be the most proper index in showing the characteristic of the self-balanced effect. The size of the connecting pipes was determined as the same as that for the nonbalanced inlet/outlet size, which is calculated by the predetermined R_0 and maximum system flow rate.

Table 12. Estimation table of storage efficiencies and effective temperature differences composed of significant factors.

Non-balanced Type			Self-balanced Type		
Mean value ± Confident Interval	Storage Efficiencies η_s 0.982±0.143	Effective Temperature Difference $\Delta\theta_e=\eta_s\cdot\Delta\theta_0$ 8.38±1.58°C	Mean value ± Confident Interval	Storage Efficiencies η_s 0.682±0.170	Effective Temperature Difference $\Delta\theta_e=\eta_s\cdot\Delta\theta_0$ 5.81±1.07°C
A	0.062**	0.46*	B	−0.080**	−0.42**
B	0.047**	0.49*	D	0.065**	0.50**
C	0.056**	0.43*	E	–	0.99**
D	0.125**	0.97**	F	−0.071**	0.54**
E	0.127**	1.82**	G	−0.053*	−0.44*
F	–	1.28**	H	0.190**	2.24**
G	−0.045**	–	I	0.117**	1.00**
H	0.126**	1.88**	J	0.058**	0.88**
I	0.030*	–	K	0.078**	0.55**
J	–	0.52*	D×E	0.057**	0.63**
A×C	−0.048**	−0.43*	D×F	−0.068**	−0.52**
A×D	0.043**	–	E×H	–	0.69**
A×I	−0.105**	–	G×I	0.064**	0.57**
D×E	−0.092**	−0.65**	J×K	0.115**	0.96**
D×F	−0.039*	–			
E×G	0.032*	–			
E×H	−0.043**	0.42*			
F×G	0.058**	–			
G×I	0.030*	–			

Note. 1. Reversed sign (+,−) should be applied to the second level.
2. Reversed sign should be applied to the combination of different levels of a couple of factors in case of interactions.
3. Significant level:
** 1% * 5%

The storage efficiency, η_s, is defined by Eq. (31);

$$\eta_s = H_s / \Delta\theta_0 V \tag{31}$$

where the H_s is the daily heat stored in the tank, $\Delta\theta_0$ is the nominal temperature difference of the cooling/heating coil, and V is the total volume of water. A detailed explanation of the storage efficiency and the nominal temperature difference is given in Part 1. The effective temperature difference, $\Delta\theta_e$, is defined as $\Delta\theta_0 \cdot \eta_s$ so that $\Delta\theta_e$ is the dominant value in determining the tank volume. Unlike the preceding two papers, $\Delta\theta_0$ varies according to the combination of levels of factor E and F.

Table 12 shows the results of ANOVA (analysis of variance) and the factorial effects for each significant factor and the interactions between a few significant factors. As already forecast qualitatively through results of model experiments and numerical simulations, the primary subheader shows a positive effect as the R-value is not small enough and the number of connecting pipes is not significant, while CDT, the operation schedule, I/O style, and particularly the R-value and LDTR2 show significant effect. However, the negative effects of the temperature difference in CWV systems may look curious, but they are recovered by advantageously applying interaction effects and offer a favorable situation. When the nominal temperature difference, $\Delta\theta_0$, varies, it is not easy to understand the ultimate performance by the storage efficiency. Then it should be noted again that

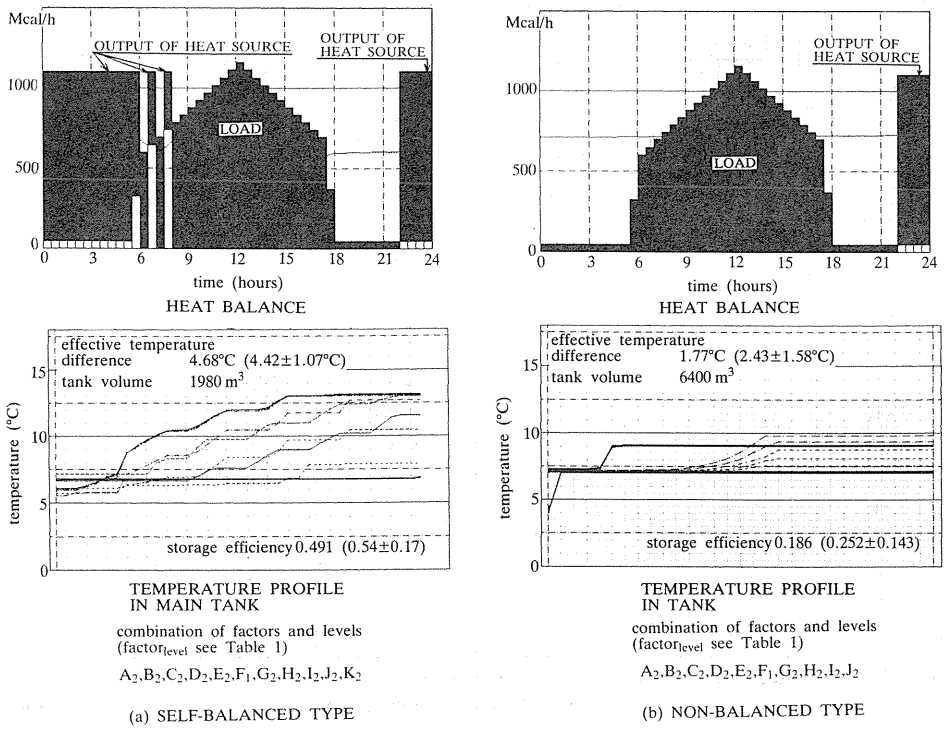

Fig. 33. Comparison of storage performance between self-balanced and non-balanced temperature stratified tank.

the final judgement is done by effective temperature difference. According to the second column for the self-balanced tanks in Table 12, it is clearly shown that the temperature difference of a CWV system gives significant positive effect to the effective temperature difference of both types of temperature-stratified tanks.

It is quite interesting to compare the self-balanced and the nonbalanced to obtain the characteristic ideas for both prototypes in this table. The original object to exclude the unfavorable effect due to the CWV system on the nonbalanced temperature-stratified tank was thus realized, noting the fact that the factorial effect, E, was insignificant in the self-balanced type. Note that the results of the nonbalanced type of efficiency shown in Table 12 seem to show a slight difference from those in Part 2 due to the difference of scale of the experimental design, that is, the number of factors and levels. Fundamentally, no contradictions exist between the two. Fig. 33 shows a comparison of the simulation results of the temperature profile, heat balance, and storage efficiencies for two cases between nonbalanced and balanced storage consisting of single tank, which exhibits peculiar differences of characteristics between the two. The result for the nonbalanced type in the figure is the worst one among 32 computed cases. Heat balance is not obtained in this case due to the extreme inefficiency, while the balanced type recovers efficiency even in such an unfavorable combination of design/operation conditions.

Conclusion

1. The basic design concept was introduced, and storage efficiency, which is expressed in the volumetric sense, was explained using the temperature profile.
2. HVAC and its heat source system with water thermal storage should be equipped with proper controls both in the primary and secondary circuits. A standard system was introduced and defined by a diagram.
3. The three prototypes of water thermal storage presented in this paper, are multi-connected complete mixing tanks, single or multi-connected temperature-stratified tanks, and self-balanced temperature-stratified tanks.
4. Use of computerized system simulation combined with the orthogonal array of design of experiment is very useful in examining the significance of factors and their complicated interactions. The estimation table and the figures of storage efficiency for three prototypes were prepared therewith.
5. Numerical simulations and experiments clarified the mixing structure in the three prototypes.
6. The each tank in the multi-connected tanks which consists of more than fifteen tanks may be considered as complete mixing due to small temperature difference and comparatively high water velocity.
7. A theoretical mixing model for the temperature-stratified storage tank was developed as the combination of complete mixing and piston flow.
8. Empirical equations for the model parameters of temperature stratified tank were derived from many experiments under the stepwise temperature input. The Archimedean Number defined at the water inlet has the dominant effect on the mixing structure of the temperature stratified tanks. The mixing model was further extended to be applied to variable input conditions encountered in actual HVAC systems.

9. A new idea to ensure temperature stratification for any variable input introduced into a thermal storage tank, in which the balanced effect, which is the natural water circulation between the main tank and subheaders, forced by buoyancy, eliminates the danger of temperature stratification decay without any forced energy, has been established.
10. The typical characteristics of balanced storage, the mixing model of which are the combination of complete mixing and piston flow with one-dimensional diffusion for buoyant inflow at surface boundary, as introduced in Part 2, complete mixing for mixing inflow due to buoyancy/gravity, and the balanced effect, were made clear through experiments and numerical calculations. These include the effect of the Archimedean number based on the tank height, the inlet velocity, and the diameter of connecting pipe, which thoroughly explained the character of temperature stratification with the self-balanced effect.
11. Even under the most adverse conditions of CWV systems with low temperature difference, the storage efficiency and effective temperature difference remained comparatively high, in case of self-balanced temperature-stratified prototype. Thus, the last prototype made the temperature-stratified water thermal storage realistic, stable, and applicable to any kind of variable input.
12. The design method using prepared estimation tables of storage efficiency was introduced in order for engineers accustomed to conventional systems to recognize the peculiarities of the water thermal storage system.

Nomenclature

A = maximum area covered between the highest temperature profile and the lowest temperature profile in the storage tank
A_0 = reference area of temperature profile to define storage efficiency
A_{con_j} = area of connecting pipe j [m^2]
Ar = Archimedean number (defined in text) [−]
Ar_h = Archimedean number at the water inlet to the tank based on the tank height, L, as the representative length ($=Lg\Delta\rho/\rho u^2$) [−]
Ar_{in} = Archimedean number at the water inlet to the tank based on the diameter of inlet pipe, d_0, as the representative length ($=d_0 g\Delta\rho/\rho u^2$) [−]
COP = Coefficient of performance of heat pump [−]
COP' = lowered value of COP due to the temperature change [−]
c = specific heat [Mcal/kg°C]
d_{con_j} = diameter of the connecting pipe j (in case of one subheader) [m]
$d_{con_{j,k}}$ = diameter of the j th connecting pipe j from k th subheader (in case of plural subheaders) [m]
d_{e_j} = diameter equivalent to those of connecting pipes from plural subheaders at level j [m]
d_0 = inlet diameter (pipe inlet) [m]
d_s = inlet vertical width (full slot inlet) [m]
$F_{o,in}$ = system flow [m^3/s]
G = capacity of heating water or chilled water generator such as heat pump, heat exchanger, etc. [MJ/h] [Mcal/h]

G_0 = initial value of G in manual calculation [MJ/h] [Mcal/h]
G_r = Grashof number [−]
g = gravity acceleration [m/s^2]
H = daily total heat load including heat loss of storage tank [MJ/day] [Mcal/day]
H_d = daily total heat load without heat loss of storage tank [MJ/day] [Mcal/day]
H_s = daily heat load to be stored [MJ/day] [Mcal/day]
H_c = total daily heat load of CWV system [MJ/day] [Mcal/day]
H_v = total daily heat load of VWV system [MJ/day] [Mcal/day]
K_i = coefficient of heat transfer of i-th surface in a corresponding tank to calculate heat loss or gain through the tank [MJ/m^{2}h°C] [Mcal/m^{2}h°C]
L = depth of tank=tank height [m]
L_{conj} = length of connecting pipe j [m]
l_m = length of complete mixing region [m]
l_0 = imaginary initial value of l_m [m]
P = effective volume ratio [−]
$\Delta P(z,t)$ = pressure difference between subheader tank and main tank at the depth z and time t [Pa]
P_s = static pressure at the top of the subheader tank [Pa]
ΔP_{L_j} = pressure drop at connecting pipe j [Pa]
Q = flow rate [m^3/s]
Q_R = water flow rate into the tank from chiller [m^3/s]
Q_i = water flow rate through i-th HVAC system at the time of peak load as a whole system [m^3/s]
$Q_{j,k}$ = flow rate from j th connecting pipe of k th subheader [m^3/s]
$Q(t)$ = hourly heat load [MJ/h] [Mcal/h]
Q_{loss} = averaged hourly total heat loss [MJ/h] [Mcal/h]
q_{loss} = heat loss/gain through the tank wall [MJ/h] [Mcal/h]
$q_{loss,T}$ = heat loss/gain through the tank wall at the time step T in finite difference equation [MJ/h] [Mcal/h]
R = dimensionless depth of complete mixing region [−]
Re = Reynolds number [−]
R_K = constant of model [−]
R_0 = initial value of R [−]
T = time or time length [s] [h]
ΔT = time interval for calculation [s] [h]
T^* = dimensionless time [−]
ΔT^* = dimensionless time interval [−]
T_{off} = OFF-time of generator [hrs]
T_{on} = ON-time of generator [hrs]
T_i, T_j = times pertains to temperature profile of the storage tank [hrs]
t_0 = basic storage temperature or design outlet temperature from generator [°C]
t_i = design inlet temperature to generator [°C]
t_1 = the lowest (or the highest, in case of heating,) allowable inlet temperature to generator [°C]
t_2 = the highest (or the lowest, in case of heating,) allowable delivery temperature to HVAC coils [°C]
t_r = temperature of returning water from HVAC coils at the time of peak load as a whole, $t_r=t_0+\Delta\theta_0$ [°C]

t_{r1} = the outlet temperature from generator at the time of inlet temperature of t_1 [°C]
t_{r2} = the outlet temperature or return temperature from HVAC coils at the time of delivery temperature t_2 [°C]
Δt_1 = limit temperature difference at the primary or generator side, $t_r - t_1$ [°C]
Δt_2 = limit temperature difference at the secondary or HVAC side, $t_2 - t_0$ [°C]
Δt_h = limit temperature difference defined another way at the generator inlet side, $t_i - t_1$ [°]
$\Delta t_h'$ = limit temperature difference defined at generator outlet side, $t_0 - t_{r1}$
t_w = mean water temperature of storage tank for a peak load day to calculate Q_{loss} [°C]
U = velocity at cross section of tank [m/s]
u = inlet velocity to the tank [m/s]
u_{ej} = equivalent velocity in connecting pipe j assuming that plural inputs from more than two subheaders are synthesized to one [m/s]
u_{con_j} = velocity in the connecting pipe j [m/s]
V = tank volume [m^3]
V_0 = nominal total tank volume calculated by $H_s/c\rho\Delta\theta_0$ [m^3]
V_{max} = allowable maximum tank volume from the structural point of view [m^3]
z = depth from water surface [m]
z_j = vertical distance of connecting pipe j from water surface [m]
Δz = spatial step of computation [m]
z^* = dimensionless depth [−]

Greek Letters

α = safety factor to calculate tank volume [−]
ε = averaged load factor of generator [−]
ζ_j = coefficient of resistance at connecting pipe j [−]
ζ_1 = resistance coefficient at the pie inlet [−]
ζ_2 = resistance coefficient at the pie outlet [−]
η_s = storage efficiency [−]
$\Delta\eta_i$ = factorial effects of storage efficiency [−]
θ = water temperature [°C]
θ_c = actual outlet temperature from generator [°C]
θ^* = dimensionless water temperature $= \left(\dfrac{\theta - \theta_0}{\theta_{in} - \theta_0}\right)$ [−]
θ_0 = initial water temperature in tank (temperature in the opposite end to inlet if initial temperature is not uniform) [°C]
θ_{in} = input water temperature [°C]
$\theta_{i,T}$ = water temperature in the tank i at time T in the finite difference equation [°C]
$\Delta\theta_0$ = nominal temperature difference [°C]
$\Delta\theta_e$ = effective temperature difference, $\eta_s\Delta\theta$ [°C]
$\Delta\theta_i$ = temperature difference through the i-th HVAC coil at the time of peak load as a whole [°C]
$\Delta\theta_h$ = nominal or design temperature difference through generator [°C]
$\Delta\theta(V)$ = temperature difference between the highest and the lowest temperature profile at the tank volume V, at the peak load day [°C]
$\varkappa$ = thermal diffusivity of water [m^2/s]

λ = friction loss coefficient [−]
ρ = water density [kg/m^3]
ρ_0 = reference water density [kg/m^3]
ρ_{in} = input water density [kg/m^3]
$\Delta\rho$ = water density difference ($=|\rho_0-\rho_{in}|$) [kg/m^3]

References

1) Yanagimachi, M. 1975. "Heat storage system in Japan." *Special Bulletin International Day Program*, ASHRAE Semiannual Meeting, Atlantic City, NJ. Jan. 26–30, pp. 27–33.
2) Nakahara, N. 1967. "HVAC system and actual operating results of Osaka Broadcasting new building." *Journal of SHASE*, Vol. 41, No. 5, pp. 25–49 (Japanese).
3) Nakahara, N. 1976. "The method of increasing efficiency in actual thermal storage operation." *Journal of SHASE*, Vol. 50, No. 9, pp. 33–44 (Japanese).
4) Nakajima, Y. 1972. "Studies on thermal weighting of thermal storage tank, Pt.1–Pt.2." *Transactions of AIJ*. No. 199, pp. 37–47, No. 200, pp. 75–83 (Japanese).
5) Matsudaira, H. and Tanaka, Y. 1979. "Dynamic characteristics on a heat storage water tank Pt.1–Pt.2." *ASHRAE TRANSACTIONS*, Vol. 85, Pt.1.
6) Tamblyn, R.T. 1980. "Thermal storage: Resisting temperature blending." *ASHRAE JOURNAL*, Jan., pp. 65–70.
7) Nakahara, N., Tsujimoto, M. and Sagara, K. 1980. "Theories, analyses and methodologies for design and controls in Japanese storage practice." *Procedings of International Conference on Thermal Storage in Buildings*, Nov. 12–14, Toronto.
8) Nakahara, N. 1982. "Research and development on optimalizing control of air-conditioning system, Pt.4–Softwares and actual results on optimization for thermal storage operation and selection of heat source." *Transactions of SHASE*, No. 18, pp. 17–31 (Japanese).
9) Nakahara, N., Sagara, K. and Tsujimoto, M. 1982. "Standardization of thermal storage system and design Method of storage tank as well as heat generator capacity." *Journal of SHASE*, Vol. 56, No. 6, pp. 17–31 (Japanese).
10) Nakahara, N., Sagara, K. and Okumiya, M. 1988. "Water thermal storage tank. Part 2, Mixing model and storage estimation for temperature-stratified tank." *ASHRAE TRANSACTIONS*, Vol. 94, Pt.2.
11) Tsujimoto, M. and Boku, T. 1982. "Actual measurements of thermal properties of existing thermal storage tank." *Transactions of Lecture Meeting, SHASE*, pp. 213–216 (Japanese).
12) Yokoyama, K., Maki, E. and Ishino, H. 1979. "The simplified calculation of thermal load for energy conservation design." *Transactions of AIJ*, No. 278, pp. 113–119 (Japanese).
13) Taguchi, G. 1977. *The design of experiment.* Maruzen (Japanese).
14) Connor, W.S. and Zelen, M. 1959. *Fractional factorial experiment designs for factors at three levels, Applied math Series 54.* NBS.
15) Nakahara, N., Sagara, K. and Tsujimoto, M. 1982. "Study on heat storage water tank, Pt.3–Estimation of tank efficiency of multi-connected complete-blending tanks by system simulation using design of experiments method." *Transactions SHASE*, No. 20, pp. 59–72 (Japanese).
16) Sagara, K. and Nakahara, N. 1987. "Studies on heat storage water tank, Pt.5–Estimation of tank efficiency for stratified-type tanks by system simulation using design of experiments method." *Transactions of SHASE*, No. 35 (Japanese).
17) Nakahara, N. 1975. "Current activities of energy conservation in air conditioning in Japan." *Special Bulletin International Day Program*, ASHRAE Semiannual Meeting, Atlantic City, NJ., Jan. 26–30, pp. 48–77.
18) Yoo, J., Wildin, M.W. and Truman, C.R. 1986. "Initial formation of a thermocline in stratified thermal storage tanks." *ASHRAE Transactions*, Vol. 92, Part 2, pp. 280–292.

19) Oppel, F.J., Ghajar, A.J. and Moretti, P.M. 1986. "A numerical and experimental study of stratified thermal storage." *ASHRAE Transactions*, Vol. 92, Part 2, pp. 293–309.
20) Cochran, W.G. and Cox, G.M. 1957. *Experimental design*. New York: John Wiley.
21) Kawabata, H., Nakahara, N. and Sagara, K. 1985. "Study on characteristics of thermal storage tank. Part 14, Practical R-value model for system simulation." *Transaction of Lecture Meeting, SHASE*, pp. 521–524 (Japanese).
22) Nakahara, N. and Sagara, K. 1985. "Study on characteristics of thermal storage tank. Part 15, Evaluation on the performance of temperature stratified tank through system simulations." *Transactions of Lecture Meeting, SHASE*, pp. 529–532 (Japanese).
23) Nakahara, N. and Okumiya, M. 1984. "Optimizing of hybrid solar system design and controls." *REPORT of SPECIAL PROJECT RESEARCH on ENERGY under GRANT in AID of SCIENTIFIC RESEARCH of the MINISTRY of EDUCATION, SCIENCE and CULTURE, JAPAN*. Vol. 8, Mar., pp. 59–68.